PHYSICAL REVIEW D **95,** 054023 (2017)

η-η' mixing in large-N_c chiral perturbation theory

P. Bickert,[1] P. Masjuan,[1,2] and S. Scherer[1]

[1]*PRISMA Cluster of Excellence, Institut für Kernphysik, Johannes Gutenberg-Universität Mainz, D-55099 Mainz, Germany*

[2]*Grup de Física Teòrica, Departament de Física, Universitat Autònoma de Barcelona, and Institut de Física d'Altes Energies (IFAE), The Barcelona Institute of Science and Technology (BIST), Campus UAB, E-08193 Bellaterra (Barcelona), Spain*

(Received 20 December 2016; published 29 March 2017)

We present a calculation of the η-η' mixing in the framework of large-N_c chiral perturbation theory. A general expression for the η-η' mixing at next-to-next-to-leading order (NNLO) is derived, including higher-derivative terms up to fourth order in the 4-momentum, kinetic terms, and mass terms. In addition, the axial-vector decay constants of the η-η' system are determined at NNLO. The numerical analysis of the results is performed successively at leading order, next-to-leading order, and NNLO. We investigate the influence of one-loop corrections, Okubo-Zweig-Iizuka rule-violating parameters, and $\mathcal{O}(N_c p^6)$ contact terms.

DOI: 10.1103/PhysRevD.95.054023

I. INTRODUCTION

The mixing of states is a feature of quantum mechanics and quantum field theory, which is intimately related to the symmetries of the underlying dynamics and the eventual mechanisms leading to their breaking. Prominent examples in the realm of subatomic physics include the K^0-$\bar{K}^0$, D^0-$\bar{D}^0$, and B^0-$\bar{B}^0$ mixing and oscillations, neutrino mixing, the Cabibbo-Kobayashi-Maskawa quark-mixing matrix, and the Weinberg angle [1]. In the low-energy regime of QCD, we observe a fascinating interplay between the dynamical (spontaneous) breaking of chiral symmetry, the explicit symmetry breaking by the quark masses, and the axial $\mathrm{U}(1)_A$ anomaly. In this context, the pseudoscalar mesons η and η' represent an ideal laboratory for investigating the relevant symmetry-breaking mechanisms in QCD. For example, hadronic decays, such as $\eta^{(\prime)} \to \pi\pi\pi$ and $\eta' \to \eta\pi\pi$, test our knowledge of low-energy effective field theories (EFTs) and provide information on the light-quark masses.[1] On the other hand, electromagnetic decays such as $\eta^{(\prime)} \to \gamma^{(*)}\gamma^{(*)}$ proceed through the Adler-Bell-Jackiw anomaly [5–7]. In the case of virtual photons, the corresponding amplitudes reveal the electromagnetic structure in terms of the transition form factors.

For vanishing up-, down-, and strange-quark masses, the QCD Lagrangian has a global $\mathrm{U}(3)_L \times \mathrm{U}(3)_R$ symmetry at the classical level (see, e.g., Ref. [8] for a discussion). The transition to the quantum level results in two main features: first, the QCD vacuum is assumed to be invariant only under the subgroup $\mathrm{SU}(3)_V \times \mathrm{U}(1)_V$; i.e., the symmetry of the Lagrangian is dynamically broken in the ground state. Second, quantum corrections destroy the singlet axial-vector-current conservation; i.e., the corresponding 4-divergence has an anomaly proportional to the square of the strong coupling constant g [5–7]. As a consequence of the Goldstone theorem [9], one expects an octet of massless, pseudoscalar bosons (π, K, η_8). Because of the $\mathrm{U}(1)_A$ anomaly, the singlet eta, η_1, is massive even in the chiral limit of massless quarks [10–12]. However, invoking the large-number-of-colors ($\mathrm{L}N_c$) limit of QCD [13,14] (see, e.g., Refs. [15,16] for an introduction), i.e., $N_c \to \infty$ with $g^2 N_c$ fixed, the $\mathrm{U}(1)_A$ anomaly disappears, and the assumption of an $\mathrm{SU}(3)_V \times \mathrm{U}(1)_V$ symmetry of the ground state implies that the singlet state is also massless. In other words, in the combined chiral and $\mathrm{L}N_c$ limits, QCD at low energies is expected to generate the nonet (π, K, η_8, η_1) as the Goldstone bosons [11,17]. In the early 1980s, the chiral dynamics of the nine pseudoscalars was extensively studied within effective-Lagrangian approaches incorporating the $\mathrm{L}N_c$ limit of QCD [18–22].

Massless $\mathrm{L}N_c$ QCD is an approximation to the real world. In fact, chiral symmetry is explicitly broken by the quark masses, and SU(3) flavor symmetry is broken by the fact that the strange quark is substantially heavier than the up and down quarks [23]. As a result (of the flavor symmetry breaking), the physical η and η' states are mixed octet and singlet states. By means of an orthogonal transformation with mixing angle θ, the physical η and η' states, i.e., the mass eigenstates, are usually expressed as linear combinations of the octet and singlet states η_8 and η_1 [24]. Such a change of basis entails the diagonalization of the general quadratic mass matrix in the basis of SU(3)-octet and -singlet states, where the diagonal entries are given by the squares of the octet and the singlet masses [25,26], while the off-diagonal terms account for the SU(3)-symmetry-breaking effects [27–31].

[1]For an overview of the main topics in η and η' physics from both the theoretical and experimental sides, see Refs. [2–4] and references therein.

In the chiral limit, the $U(1)_A$ anomaly contributes only to the singlet mass [10]. As a result of the mixing, the anomaly contribution is transferred to both the η and η' states, such that the η' remains heavier than the η. A discussion of the η-η' mixing in the framework of EFT should consider both states as dynamical degrees of freedom, and, for a perturbative treatment, the respective masses should be small in comparison with a typical hadronic energy scale. Now, in the chiral limit, the η' still remains massive. For that reason, in the low-energy expansion of conventional $SU(3)_L \times SU(3)_R$ chiral perturbation theory (ChPT), the η' does not play a special role as compared to other states such as the ρ meson [27]. However, the combined chiral and LN_c limits may serve as a starting point for large-N_c chiral perturbation theory (LN_cChPT) as the EFT of QCD at low energies including the singlet field [32–40], which we will also refer to as $U(3)_L \times U(3)_R$ effective theory.[2]

In the framework of LN_cChPT, one performs a simultaneous expansion of (renormalized) Feynman diagrams in terms of momenta p, quark masses m, and $1/N_c$.[3] The three expansion variables are counted as small quantities of order [33]

$$p = \mathcal{O}(\sqrt{\delta}), \qquad m = \mathcal{O}(\delta), \qquad 1/N_c = \mathcal{O}(\delta). \quad (1)$$

The organization of the effective Lagrangian as a *simultaneous* expansion in terms of p, m, and $1/N_c$, in combination with the assignment of Eq. (1), ensures a coherent effective field theory for analyzing the low-energy properties of QCD in the limit where the number of colors, N_c, is treated as large (see Ref. [35] for details). The formulation of the effective field theory within the framework of $U(3)_L \times U(3)_R$ instead of $SU(3)_L \times SU(3)_R$ with the singlet eta as an explicit dynamical degree of freedom is a safe way to remain compatible with the large-N_c limit of QCD [41]. The corresponding power-counting rules will be discussed in Sec. II. The leading-order chiral Lagrangian is not able to reproduce the experimental result for the η and η' masses [42], and higher-order terms in the $1/N_c$ (and quark-mass) expansion must be taken into account [43]. The inclusion of loop effects in the scheme of Eq. (1) increases the order by δ^2. Thus, any calculation in this framework at the loop level needs to then be performed at least at next-to-next-to-leading order (NNLO). This order would demand the knowledge of the low-energy constants (LECs) of $\mathcal{O}(p^4)$ and of those of $\mathcal{O}(p^6)$ which are leading in $1/N_c$. The proliferation of (*a priori* unknown) LECs poses a challenge for any prediction within this theory, and information from other sources, e.g., from a matching to physical observables or lattice simulations, will be required in order to determine the LECs. For SU(3) ChPT, the LECs at $\mathcal{O}(p^4)$ are well known, and information on some of the $\mathcal{O}(p^6)$ LECs is also provided [44]. With a suitable matching, one can translate the SU(3) values into the corresponding ones within the U(3) effective theory.

Since we take higher orders of the $1/N_c$ expansion into account, terms violating the Okubo-Zweig-Iizuka (OZI) rule appear perturbatively in our calculations. They will be accompanied by a set of LECs which are rather poorly known at $\mathcal{O}(\delta)$ and basically unknown at higher orders.

If we include higher-order corrections in our effective Lagrangian, the connection between the physical η and η' states and the singlet and octet states is more complicated than a simple rotation. Furthermore, the description of the η-η' mixing with a single mixing angle θ is not appropriate to describe the experimental data, and also the axial-vector decay constants of the η-η' system [at next-to-leading order (NLO)] cannot be described by a simple rotation with angle θ. This problem was solved by invoking a mixing scheme with two different angles, the so-called two-angle mixing scheme [45,46]. In recent years, the use of the two-angle scheme has been very popular and resulted in well-established phenomenological determinations of the mixing [45–52], a procedure that can also be extended to include an eventual gluonium content of these pseudoscalars (see, e.g., Refs. [53–55]).

This work is organized as follows. In Sec. II, we describe the effective field theory we will consider for our calculation by specifying the Lagrangian and the power counting. In Sec. III, we present the calculation of the mixing angles at NNLO. Section IV deals with the η and η' decay constants. In Sec. V, we elaborate on the numerical analysis of the mixing, decay constants, and pseudoscalar masses with different input sets of LECs. Finally, in Sec. VI, we conclude with a few remarks and an outlook of possible future work.

II. LAGRANGIANS AND POWER COUNTING

The most general Lagrangian of LN_cChPT is organized as an infinite series in terms of derivatives, quark-mass terms, and, implicitly, powers of $1/N_c$, with the scaling behavior given in Eq. (1),

$$\mathcal{L}_{\text{eff}} = \mathcal{L}^{(0)} + \mathcal{L}^{(1)} + \mathcal{L}^{(2)} + \cdots, \quad (2)$$

where the superscripts (i) denote the order in δ. The rules leading to the assignments of these orders will be explained below. The properties of the building blocks are defined in Appendix A.

The dynamical degrees of freedom are collected in the unitary 3×3 matrix

$$U(x) = \exp\left(i\frac{\phi(x)}{F}\right), \quad (3)$$

where the Hermitian 3×3 matrix

[2]For the sake of notational brevity, from now on, we will use the terminology SU(3) and U(3) ChPT instead of $SU(3)_L \times SU(3)_R$ and $U(3)_L \times U(3)_R$ ChPT, respectively.

[3]It is understood that dimensionful variables need to be small in comparison with an energy scale.

$$\phi=\sum_{a=0}^{8}\phi_a\lambda_a=\begin{pmatrix}\pi^0+\frac{1}{\sqrt{3}}\eta_8+\sqrt{\frac{2}{3}}\eta_1 & \sqrt{2}\pi^+ & \sqrt{2}K^+\\ \sqrt{2}\pi^- & -\pi^0+\frac{1}{\sqrt{3}}\eta_8+\sqrt{\frac{2}{3}}\eta_1 & \sqrt{2}K^0\\ \sqrt{2}K^- & \sqrt{2}\bar{K}^0 & -\frac{2}{\sqrt{3}}\eta_8+\sqrt{\frac{2}{3}}\eta_1\end{pmatrix} \tag{4}$$

contains the pseudoscalar octet fields and the pseudoscalar singlet field η_1, the λ_a $(a=1,\ldots,8)$ are the Gell-Mann matrices, and $\lambda_0=\sqrt{2/3}\mathbb{1}$. In Eq. (3), F denotes the pion-decay constant in the three-flavor chiral limit[4] and is counted as $F=\mathcal{O}(\sqrt{N_c})=\mathcal{O}(1/\sqrt{\delta})$.[5] The pseudoscalar fields ϕ_a $(a=0,\ldots,8)$ count as $\mathcal{O}(\sqrt{N_c})$ such that the argument of the exponential function is $\mathcal{O}(\delta^0)$ and, thus, $U=\mathcal{O}(\delta^0)$. Besides the dynamical degrees of freedom of Eq. (4), the effective Lagrangian also contains a set of external fields (s,p,l_μ,r_μ,θ). The fields s, p, l_μ, and r_μ are Hermitian, color-neutral 3×3 matrices coupling to the corresponding quark bilinears, and θ is a real field coupling to the winding-number density [27]. A nonvanishing constant value for θ would give rise to parity violation and CP violation in the strong interactions, resulting in, e.g., an electric dipole moment of the neutron [56]. However, the present empirical information on this quantity suggests that θ is tiny [57], and, therefore, while displaying the θ dependence in the Lagrangians, we set $\theta=0$ in our calculations. The external scalar and pseudoscalar fields s and p are combined in the definition $\chi\equiv 2B(s+ip)$ [27]. The LEC B is related to the scalar singlet quark condensate $\langle\bar{q}q\rangle_0$ in the three-flavor chiral limit and is of $\mathcal{O}(N_c^0)$.

In general, applying the power counting of Eq. (1) to the construction of the effective Lagrangian in the LN_c framework involves two ingredients. On the one hand, there is the momentum and quark-mass counting, which proceeds as in conventional SU(3) ChPT [27]: (covariant) derivatives count as $\mathcal{O}(p)$, χ counts as $\mathcal{O}(p^2)$, etc. (see Table I). We denote the corresponding chiral order by D_p. The discussion of the U(3) case results in essentially three major modifications in comparison with SU(3) [33–35]: first, the determinant of U is no longer restricted to have the value 1; second, additional external fields appear; and third, the conventional structures of SU(3) ChPT will be multiplied by coefficients which are functions of the linear combination $(\psi+\theta)$, where $\psi\equiv\sqrt{6}\eta_1/F$ such that $\det(U)=\exp(i\psi)$. According to Eqs. (A1), the sum $(\psi+\theta)$ remains invariant under chiral $\mathrm{U}(3)_L\times\mathrm{U}(3)_R$ transformations. For example, denoting the SU(3) matrix of ordinary ChPT by $\hat{U}$, the leading-order Lagrangian reads [27]

$$\mathcal{L}_2=\frac{F^2}{4}\langle D_\mu\hat{U}D^\mu\hat{U}^\dagger\rangle+\frac{F^2}{4}\langle\chi\hat{U}^\dagger+\hat{U}\chi^\dagger\rangle,$$

where the symbol $\langle\rangle$ denotes the trace over flavor indices and the covariant derivatives are defined in Eqs. (A2). This expression is replaced by [34]

$$W_1\langle D_\mu UD^\mu U^\dagger\rangle+W_2\langle\chi U^\dagger+U\chi^\dagger\rangle, \tag{5}$$

where W_1 and W_2 are functions of $(\psi+\theta)$ and are also referred to as potentials [35]. In the limit $N_c\to\infty$, these functions reduce to constants [33]. However, for N_c finite, the functions may be expanded in $(\psi+\theta)$ with well-defined assignments for the LN_c scaling behavior of the expansion coefficients.

In addition to the potentials, also new additional structures which do not exist in the SU(3) case show up. For example, in ordinary ChPT, one finds for the trace $\langle D_\mu\hat{U}\hat{U}^\dagger\rangle=0$ [8], whereas in the U(3) case, one has

TABLE I. Power-counting rules in LN_cChPT. a) The inverse of the singlet η_1 propagator is of order $1/N_c$ and p^2. b) The assignment i in $\mathcal{L}^{(i)}$ receives contributions from both $1/N_c$ and p^2. Recall that powers $(\psi+\theta)^n$ come with expansion coefficients of $\mathcal{O}(N_c^{-n})$ even though we count $(\psi+\theta)$ as $\mathcal{O}(1)$.

Quantity	N_c	p	δ
Momenta/derivatives p/∂_μ	1	p	$\delta^{\frac{1}{2}}$
$1/N_c$	N_c^{-1}	1	δ
Quark masses m	1	p^2	δ
Dynamical fields ϕ_a $(a=1,\ldots,8)$	$\sqrt{N_c}$	1	$\delta^{-\frac{1}{2}}$
Dynamical field ψ	1	1	1
External field θ	1	1	1
External currents v_μ and a_μ	1	p	$\delta^{\frac{1}{2}}$
External fields s and p	1	p^2	δ
Pion-decay constant F (chiral limit)	$\sqrt{N_c}$	1	$\delta^{-\frac{1}{2}}$
Topological susceptibility τ	1	1	1
$M_{\eta'}^2$ (chiral limit)	N_c^{-1}	1	δ
Octet-meson propagator	1	p^{-2}	δ^{-1}
Singlet-η_1 propagator (chiral limit)	a)	a)	δ^{-1}
Loop integration	1	p^4	δ^2
k-meson vertex from $\mathcal{L}^{(i)}$	b)	b)	$\delta^{i+k/2}$

[4]Here, we deviate from the often-used convention of indicating the *three*-flavor chiral limit by a subscript 0.

[5]Consider a generic quark bilinear of the type $\bar{q}\Gamma Fq$, with Γ and F standing for matrices in Dirac and flavor space, respectively, and a summation over color indices implied. In the LN_c limit of QCD, the matrix element for any such quark bilinear to create a meson from the vacuum scales like $\sqrt{N_c}$ [14].

$$\langle D_\mu U U^\dagger \rangle = i D_\mu \psi, \tag{6}$$

giving rise to a new term of the type $-W_4 D_\mu \psi D^\mu \psi$ [34].

The LN_c behavior can be determined by using the following rules (see Refs. [34,35] for a detailed account). In the LN_c counting, the leading contribution to a quark correlation function is given by a single flavor trace and is of order N_c [13,14,16]. In general, diagrams with r quark loops and thus r flavor traces are of order N_c^{2-r}. Terms without traces correspond to the purely gluonic theory and count at leading order as N_c^2. This argument is transferred to the level of the effective Lagrangian; i.e., single-trace terms are of order N_c, double-trace terms are of order unity, etc.[6] In other words, we need to identify the number $N_{\rm tr}$ of flavor traces. In particular, because of Eq. (6), the expression $D_\mu \psi$ implicitly involves a flavor trace (see footnote 7 of Ref. [35]). Furthermore, when expanding the potentials, each power $(\psi + \theta)^n$ is accompanied by a coefficient of order $\mathcal{O}(N_c^{-n})$. The reason for this assignment is the fact that, in QCD, the external field θ couples to the winding-number density with strength $1/N_c$. In a similar fashion, $D_\mu \theta$ (as well as multiple derivatives) are related to expressions with $\mathcal{O}(N_c^{-1})$.[7] Denoting the number of $(\psi + \theta)$ and $D_\mu \theta$ terms by N_θ, the LN_c order reads [34,35]

$$D_{N_c^{-1}} = -2 + N_{\rm tr} + N_\theta. \tag{7}$$

The combined order of an operator is then given by

$$D_\delta = \frac{1}{2} D_p + D_{N_c^{-1}}. \tag{8}$$

In particular, using Eq. (8) allows us to identify the LN_c scaling behavior of the LEC multiplying the corresponding operator.

The leading-order Lagrangian contains three LECs, namely, F, B, and τ, and is given by [33,35]

$$\mathcal{L}^{(0)} = \frac{F^2}{4} \langle D_\mu U D^\mu U^\dagger \rangle + \frac{F^2}{4} \langle \chi U^\dagger + U \chi^\dagger \rangle - \frac{1}{2} \tau (\psi + \theta)^2. \tag{9}$$

Comparing with Eq. (5), we identify

$$\frac{F^2}{4} = W_1(0) = W_2(0)$$

as the leading-order term of the expansion of the functions W_1 and W_2 which, because of parity, are even functions. On the other hand, the last term of Eq. (9) originates from the second-order term of the expansion of W_0. The constant $\tau = \mathcal{O}(N_c^0)$ is the topological susceptibility of the purely gluonic theory [33]. Counting the quark mass as $\mathcal{O}(p^2)$, the first two terms of $\mathcal{L}^{(0)}$ are of $\mathcal{O}(N_c p^2)$, while the third term is of $\mathcal{O}(N_c^0)$; i.e., all terms are of $\mathcal{O}(\delta^0)$. The leading-order Lagrangian of Eq. (9) corresponds to the effective Lagrangians of Refs. [18–20].[8] Note that Refs. [19] and [20] explicitly display the N_c dependence of the last term in Eq. (9), whereas we absorb it in the definition of the parameter τ. Reference [22] also discusses a few next-to-leading terms in $1/N_c$ and the quark masses. The effective Lagrangians of Refs. [18–22] are meant to be used at the tree level, whereas LN_cChPT also contains loop corrections. Applying the external-field method of Gasser and Leutwyler [27] implies that the global chiral symmetry is promoted to a local symmetry. As a result, Eq. (9) contains covariant derivatives in place of ordinary derivatives in the effective-Lagrangian approaches. Furthermore, at higher orders, one also encounters field strength tensors as well as derivatives thereof. Such terms are mandatory to absorb ultraviolet divergences of loop diagrams. An illustration of this point in terms of the pion electromagnetic form factor can be found in Ref. [59].

To explain the power counting of the interaction vertices, we set $r_\mu = l_\mu = 0$ and $\chi = 2BM$, where $M = \mathrm{diag}(m_u, m_d, m_s)$ denotes the quark-mass matrix. For this case, the leading-order Lagrangian contains only even powers of the pseudoscalar fields. Expanding the first two terms of Eq. (9) in terms of the pseudoscalar fields results in Feynman rules for the *interaction* vertices of the order $p^2 N_c^{1-k/2}$, where $k = 4, 6, \ldots$ is the number of interacting pseudoscalar fields [35]. The dependence on N_c and p originates from the powers of F and the two derivatives, respectively. When discussing QCD Green functions of, say, pseudoscalar quark bilinears, there will be a factor $BF = \mathcal{O}(\sqrt{N_c})$ at each external source (see Sec. 4. 6. 2 of Ref. [60]), such that an n-point function is of the order $p^2 N_c$. Taking $\phi_a = \mathcal{O}(\sqrt{N_c})$, the interaction Lagrangians count as $\mathcal{O}(p^2 N_c)$, which is consistent with referring to the Lagrangian as $\mathcal{O}(\delta^0)$, with the leading-order contributions of quark loops being $\mathcal{O}(N_c)$ and the leading chiral order being $\mathcal{O}(p^2)$. On the other hand, it is also consistent with the expectation of the effective meson vertices containing k external lines being of the order $N_c^{1-k/2}$ [14].

The NLO Lagrangian $\mathcal{L}^{(1)}$ was constructed in Refs. [33–35] and receives contributions of $\mathcal{O}(N_c p^4)$, $\mathcal{O}(p^2)$, and $\mathcal{O}(N_c^{-1})$. The terms that are of the same structure as those in $\mathcal{L}^{(0)}$ may be absorbed in the coupling constants F, B, and τ [35]. In particular, τ now has to be distinguished from the topological susceptibility of gluodynamics. We only display the terms relevant for our

[6] When applying these counting rules, one has to account for the so-called trace relations connecting single-trace terms with products of traces (see, e.g., Appendix A of Ref. [58]).

[7] Note that we do not directly book the quantities $(\psi + \theta)$ or $D_\mu \theta$ as $\mathcal{O}(N_c^{-1})$ but rather attribute this order to the coefficients coming with the terms.

[8] See Eqs. (7), (10), and (2.22) of Refs. [18,19], and [20], respectively.

calculation; in particular, we set $v_\mu \equiv (r_\mu + l_\mu)/2 = 0$ and keep only $a_\mu \equiv (r_\mu - l_\mu)/2$, which is needed for the calculation of the axial-vector-current matrix elements,

$$\begin{aligned}\mathcal{L}^{(1)} &= L_5\langle D_\mu U D^\mu U^\dagger(\chi U^\dagger + U\chi^\dagger)\rangle \\ &\quad + L_8\langle \chi U^\dagger \chi U^\dagger + U\chi^\dagger U\chi^\dagger\rangle + \frac{F^2}{12}\Lambda_1 D_\mu\psi D^\mu\psi \\ &\quad - i\frac{F^2}{12}\Lambda_2(\psi+\theta)\langle \chi U^\dagger - U\chi^\dagger\rangle + \cdots, \end{aligned} \tag{10}$$

where

$$D_\mu\psi = \partial_\mu\psi - 2\langle a_\mu\rangle, \tag{11}$$

$$D_\mu\theta = \partial_\mu\theta + 2\langle a_\mu\rangle \tag{12}$$

and the ellipsis refers to the suppressed terms. The first two terms of $\mathcal{L}^{(1)}$ count as $\mathcal{O}(N_c p^4)$ and are obtained from the standard SU(3) ChPT Lagrangian of $\mathcal{O}(p^4)$ [27] by retaining solely terms with a single trace and keeping only the constant terms of the potentials. With $D_p = 4$ and $D_{N_c^{-1}} = -1$, Eq. (8) implies that L_5 and L_8 are of $\mathcal{O}(N_c)$. According to Eq. (11), the expression $D_\mu\psi D^\mu\psi$ implicitly involves two flavor traces (see footnote 7 of Ref. [35]), with the result that the corresponding term is $\mathcal{O}(N_c^0)$. Since $F = \mathcal{O}(\sqrt{N_c})$, the coupling Λ_1 scales as $\mathcal{O}(N_c^{-1})$ and has to vanish in the LN_c limit. Finally, the structure proportional to Λ_2 is the leading-order term of the expansion of the potential W_3. With $D_p = 2$ and $D_{N_c^{-1}} = 0$ ($N_{\rm tr} = N_\theta = 1$), the LEC Λ_2 scales as $\mathcal{O}(N_c^{-1})$.

The SU(3) Lagrangian of $\mathcal{O}(p^6)$ was discussed in Refs. [58,61–63], and the generalization to the U(3) case has recently been obtained in Ref. [64]. For the present purposes, at NNLO, the relevant pieces of $\mathcal{L}^{(2)}$ can be split into three different contributions of $\mathcal{O}(N_c^{-1}p^2)$, $\mathcal{O}(p^4)$, and $\mathcal{O}(N_c p^6)$, respectively,

$$\mathcal{L}^{(2,N_c^{-1}p^2)} = -\frac{F^2}{4}v_2^{(2)}(\psi+\theta)^2\langle \chi U^\dagger + U\chi^\dagger\rangle, \tag{13}$$

$$\begin{aligned}\mathcal{L}^{(2,p^4)} &= L_4\langle D_\mu U D^\mu U^\dagger\rangle\langle \chi U^\dagger + U\chi^\dagger\rangle + L_6\langle \chi U^\dagger + U\chi^\dagger\rangle^2 \\ &\quad + L_7\langle \chi U^\dagger - U\chi^\dagger\rangle^2 + iL_{18}D_\mu\psi\langle \chi D^\mu U^\dagger - D^\mu U\chi^\dagger\rangle \\ &\quad + iL_{25}(\psi+\theta)\langle \chi U^\dagger\chi U^\dagger - U\chi^\dagger U\chi^\dagger\rangle \\ &\quad + iL_{46}D_\mu\theta\langle D^\mu U U^\dagger(\chi U^\dagger + U\chi^\dagger)\rangle \\ &\quad + iL_{53}\partial_\mu D^\mu\theta\langle \chi U^\dagger - U\chi^\dagger\rangle + \cdots, \end{aligned} \tag{14}$$

$$\begin{aligned}\mathcal{L}^{(2,N_c p^6)} &= C_{12}\langle \chi_+ h_{\mu\nu}h^{\mu\nu}\rangle + C_{14}\langle u_\mu u^\mu \chi_+^2\rangle \\ &\quad + C_{17}\langle \chi_+ u_\mu\chi_+ u^\mu\rangle + C_{19}\langle \chi_+^3\rangle \\ &\quad + C_{31}\langle \chi_-^2\chi_+\rangle + \cdots, \end{aligned} \tag{15}$$

where

$$\begin{aligned}\chi_\pm &= u^\dagger\chi u^\dagger \pm u\chi^\dagger u, \\ u &= \sqrt{U}, \\ u_\mu &= i[u^\dagger(\partial_\mu - ir_\mu)u - u(\partial_\mu - il_\mu)u^\dagger] = iu^\dagger D_\mu U u^\dagger, \\ h_{\mu\nu} &= \nabla_\mu u_\nu + \nabla_\nu u_\mu, \\ \nabla_\mu X &= \partial_\mu X + [\Gamma_\mu, X], \\ \Gamma_\mu &= \frac{1}{2}[u^\dagger(\partial_\mu - ir_\mu)u + u(\partial_\mu - il_\mu)u^\dagger]. \end{aligned} \tag{16}$$

The coupling $v_2^{(2)}$ of Eq. (13) scales like $\mathcal{O}(N_c^{-2})$ and originates from the expansion of the potentials of Refs. [33,35] up to and including terms of order $(\psi+\theta)^2$. The first three terms of Eq. (14) stem from the standard SU(3) ChPT Lagrangian of $\mathcal{O}(p^4)$ with two traces and are $1/N_c$ suppressed compared to the single-trace terms in Eq. (10). The remaining terms of Eq. (14) are genuinely related to the LN_c U(3) framework, since they contain interactions involving the singlet field or the singlet axial-vector current. Finally, the C_i terms of Eq. (15) are obtained from single-trace terms of the SU(3) Lagrangian of $\mathcal{O}(p^6)$ [61]. As there is, at present, no satisfactory unified nomenclature for the coupling constants, for easier reference, we choose the names according to the respective references from which the Lagrangians were taken. In our calculation, we do not include external vector fields, i.e., $v_\mu = 0$. The L_{46}, L_{53} terms in $\mathcal{L}^{(1)}$ are not needed for the calculation of the mixing. They enter, however, in the calculation of the decay constants of the axial-vector-current matrix elements.

Last but not least, we summarize the power-counting rules for a given Feynman diagram, which has been evaluated by using the interaction vertices derived from the effective Lagrangians of Eq. (2). Using the δ counting introduced in Eq. (1), we assign to any such diagram an order D which is obtained from the following ingredients: meson propagators for both octet and singlet fields count as $\mathcal{O}(\delta^{-1})$. Since meson fields are always divided by $F = \mathcal{O}(\sqrt{N_c}) = \mathcal{O}(\delta^{-\frac{1}{2}})$, a vertex with k meson fields derived from $\mathcal{L}^{(i)}$ is $\mathcal{O}(\delta^{i+k/2})$. The integration of a loop counts as δ^2. The order D is obtained by adding up the contributions of the individual building blocks. Figure 1 provides two examples of the application of the power-counting rules. Since the tree-level diagram of Fig. 1(a) consists of a single vertex

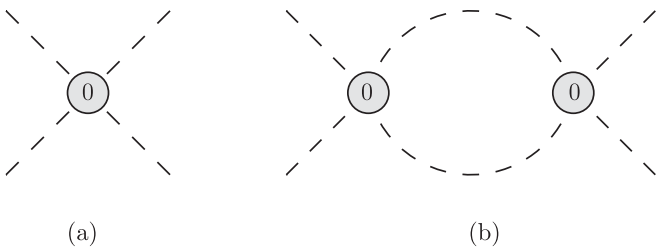

FIG. 1. Illustration of the power counting in LN_cChPT. The number 0 in the interaction blobs refers to $\mathcal{L}^{(0)}$.

derived from $\mathcal{L}^{(0)}$ with four external meson lines, it has $D = 2$. On the other hand, the one-loop diagram of Fig. 1(b) has two vertices from $\mathcal{L}^{(0)}$ with four legs, two meson propagators, and one loop: $D = 2 + 2 - 1 - 1 + 2 = 4$. As expected, the loop increases the order by two units. The power-counting rules are summarized in Table I.

III. CALCULATION OF THE MIXING ANGLE

For $m_u = m_d = \hat{m} \neq m_s$, the physical η and η' mass eigenstates are linear combinations of the mathematical octet and singlet states η_8 and η_1. Our aim is to derive a general expression for the η-η' mixing at the one-loop level up to and including NNLO in the δ counting. To that end, we start from an effective Lagrangian in terms of the octet and singlet fields and perform successive transformations, resulting in a diagonal Lagrangian in terms of the physical fields. Because of the effective-field-theory nature of our approach, the starting Lagrangian will contain higher-derivative terms up to and including fourth order in the 4-momentum. The parameters of the Lagrangian are obtained from a one-loop calculation of the self-energies using the Lagrangians and power counting of Sec. II. The Lagrangian after the transformation will have a standard "free-field" form.

Let us collect the fields η_8 and η_1 in the doublet

$$\eta_A \equiv \begin{pmatrix} \eta_8 \\ \eta_1 \end{pmatrix}. \tag{17}$$

In terms of η_A, at NNLO, the most general effective Lagrangian quadratic in η_A is of the form

$$\mathcal{L}_{\text{eff}} = \mathcal{L}_A = \frac{1}{2}\partial_\mu \eta_A^T \mathcal{K}_A \partial^\mu \eta_A - \frac{1}{2}\eta_A^T \mathcal{M}_A^2 \eta_A + \frac{1}{2}\Box \eta_A^T \mathcal{C}_A \Box \eta_A. \tag{18}$$

Note that the fields η_8 and η_1 count as $\mathcal{O}(\sqrt{N_c})$ and a single derivative counts as $\mathcal{O}(p)$. The symmetric 2×2 matrices $\mathcal{K}_A$, $\mathcal{M}_A^2$, and $\mathcal{C}_A$ can be written as

$$\mathcal{K}_A = \begin{pmatrix} 1 + k_8 & k_{81} \\ k_{81} & 1 + k_1 \end{pmatrix}, \tag{19}$$

$$\mathcal{M}_A^2 = \begin{pmatrix} M_8^2 & M_{81}^2 \\ M_{81}^2 & M_1^2 \end{pmatrix}, \tag{20}$$

$$\mathcal{C}_A = \begin{pmatrix} c_8 & c_{81} \\ c_{81} & c_1 \end{pmatrix}. \tag{21}$$

Later on, we will provide the one-loop expressions for the matrices $\mathcal{K}_A$ and $\mathcal{M}_A^2$. The matrix $\mathcal{C}_A$ is given in Eqs. (C1)–(C3) of Appendix C and is of $\mathcal{O}(p^2)$. If we were to work at leading order, only, we would have to replace

$$\mathcal{K}_A \to \mathbb{1}, \qquad \mathcal{M}_A^2 \to \mathcal{M}_A^{2\,(0)} = \begin{pmatrix} \overset{\circ}{M}{}_8^2 & \overset{\circ}{M}{}_{81}^2 \\ \overset{\circ}{M}{}_{81}^2 & \overset{\circ}{M}{}_1^2 + M_0^2 \end{pmatrix},$$
$$\mathcal{C}_A \to 0.$$

The elements of the (leading-order) mass matrix $\mathcal{M}_A^{2\,(0)}$ read

$$\overset{\circ}{M}{}_8^2 = \frac{2}{3}B(\hat{m} + 2m_s) = \frac{1}{3}(4\overset{\circ}{M}{}_K^2 - \overset{\circ}{M}{}_\pi^2), \tag{22}$$

$$\overset{\circ}{M}{}_1^2 = \frac{2}{3}B(2\hat{m} + m_s) = \frac{1}{3}(2\overset{\circ}{M}{}_K^2 + \overset{\circ}{M}{}_\pi^2), \tag{23}$$

$$M_0^2 = 6\frac{\tau}{F^2}, \tag{24}$$

$$\overset{\circ}{M}{}_{81}^2 = -\frac{2\sqrt{2}}{3}B(m_s - \hat{m}) = -\frac{2\sqrt{2}}{3}(\overset{\circ}{M}{}_K^2 - \overset{\circ}{M}{}_\pi^2), \tag{25}$$

where $\overset{\circ}{M}{}_K^2 = B(\hat{m} + m_s)$ and $\overset{\circ}{M}{}_\pi^2 = 2B\hat{m}$ are the leading-order kaon and pion masses squared, respectively, and M_0^2 denotes the $\mathrm{U}(1)_A$ anomaly contribution to the η_1 mass squared. The mixing already shows up at leading order, because the mass matrix $\mathcal{M}_A^2$ is nondiagonal at that order. The "kinetic" matrix $\mathcal{K}_A$ receives NLO and NNLO corrections. Finally, the last term in Eq. (18), containing higher derivatives of η_A, originates from the C_{12} term of the $\mathcal{O}(\delta^2)$ Lagrangian in Eq. (15).

Our first step is to perform a field redefinition to get rid of the higher-derivative structure in Eq. (18) [65,66],

$$\eta_A = \left(\mathbb{1} + \frac{1}{2}\mathcal{C}_A \Box\right)\eta_B. \tag{26}$$

The entries of $\mathcal{C}_A$ are of $\mathcal{O}(p^2)$, and the d'Alembertian operator counts as $\mathcal{O}(p^2)$. The field transformation is constructed such that, after inserting Eq. (26) into Eq. (18), the last term is canceled by a term originating from the first term in Eq. (18). Moreover, we obtain additional terms originating from the "mass term" of Eq. (18) which now contribute to the new kinetic matrix. Finally, we neglect any term generated by the field transformation which is beyond the accuracy of a NNLO calculation. Using the relation $\phi\Box\phi = \partial_\mu(\phi\partial^\mu\phi) - \partial_\mu\phi\partial^\mu\phi$ for the components of η_B, and neglecting total-derivative terms, the Lagrangian after the first field redefinition is of the form

$$\mathcal{L}_B = \frac{1}{2}\partial_\mu \eta_B^T \mathcal{K}_B \partial^\mu \eta_B - \frac{1}{2}\eta_B^T \mathcal{M}_B^2 \eta_B, \tag{27}$$

where

$$\mathcal{K}_B = \mathcal{K}_A + \frac{1}{2}\begin{pmatrix} 2c_8\overset{\circ}{M}_8^2 + 2c_{81}\overset{\circ}{M}_{81}^2 & (c_1+c_8)\overset{\circ}{M}_{81}^2 + c_{81}(\overset{\circ}{M}_1^2 + M_0^2 + \overset{\circ}{M}_8^2) \\ (c_1+c_8)\overset{\circ}{M}_{81}^2 + c_{81}(\overset{\circ}{M}_1^2 + M_0^2 + \overset{\circ}{M}_8^2) & 2c_1(\overset{\circ}{M}_1^2 + M_0^2) + 2c_{81}\overset{\circ}{M}_{81}^2 \end{pmatrix}$$
$$= \begin{pmatrix} 1+\delta_8^{(1)}+\delta_8^{(2)} & \delta_{81}^{(1)}+\delta_{81}^{(2)} \\ \delta_{81}^{(1)}+\delta_{81}^{(2)} & 1+\delta_1^{(1)}+\delta_1^{(2)} \end{pmatrix}, \tag{28}$$

where $\delta_j^{(i)}$ denotes corrections of $\mathcal{O}(\delta^i)$. The entries of the mass matrix $\mathcal{M}_B^2 = \mathcal{M}_A^2$ are given by

$$M_8^2 = \overset{\circ}{M}_8^2 + \Delta M_8^{2(1)} + \Delta M_8^{2(2)}, \tag{29}$$

$$M_1^2 = M_0^2 + \overset{\circ}{M}_1^2 + \Delta M_1^{2(1)} + \Delta M_1^{2(2)}, \tag{30}$$

$$M_{81}^2 = \overset{\circ}{M}_{81}^2 + \Delta M_{81}^{2\,(1)} + \Delta M_{81}^{2\,(2)}, \tag{31}$$

where $\Delta M_j^{2(i)}$ denotes corrections of $\mathcal{O}(\delta^i)$.

The next step consists of diagonalizing the kinetic matrix $\mathcal{K}_B$ in Eq. (28) up to and including $\mathcal{O}(\delta^2)$ through the field redefinition

$$\eta_B = \sqrt{Z}\eta_C, \tag{32}$$

such that

$$\sqrt{Z}^T \mathcal{K}_B \sqrt{Z} = \mathbb{1}. \tag{33}$$

Writing $\mathcal{K}_B$ as

$$\mathcal{K}_B = \mathbb{1} + K^{(1)} + K^{(2)}$$

and making an ansatz for the symmetric matrix $\sqrt{Z}$ of the form

$$\sqrt{Z} = \mathbb{1} + \sqrt{Z}^{(1)} + \sqrt{Z}^{(2)},$$

we obtain from Eq. (33) the conditions

$$2\sqrt{Z}^{(1)} + K^{(1)} = 0 \Rightarrow \sqrt{Z}^{(1)} = -\frac{1}{2}K^{(1)},$$

and

$$2\sqrt{Z}^{(2)} + K^{(2)} + \sqrt{Z}^{(1)2} + \sqrt{Z}^{(1)}K^{(1)} + K^{(1)}\sqrt{Z}^{(1)} = 0$$
$$\Rightarrow \sqrt{Z}^{(2)} = -\frac{1}{2}K^{(2)} + \frac{3}{8}K^{(1)2}.$$

The matrix $\sqrt{Z}$ is, therefore, given by

$$\sqrt{Z} = \begin{pmatrix} 1-\frac{1}{2}\delta_8^{(1)}+\frac{3}{8}\delta_8^{(1)2}+\frac{3}{8}\delta_{81}^{(1)2}-\frac{1}{2}\delta_8^{(2)} & -\frac{1}{2}\delta_{81}^{(1)}+\frac{3}{8}\delta_1^{(1)}\delta_{81}^{(1)}+\frac{3}{8}\delta_8^{(1)}\delta_{81}^{(1)}-\frac{1}{2}\delta_{81}^{(2)} \\ -\frac{1}{2}\delta_{81}^{(1)}+\frac{3}{8}\delta_1^{(1)}\delta_{81}^{(1)}+\frac{3}{8}\delta_8^{(1)}\delta_{81}^{(1)}-\frac{1}{2}\delta_{81}^{(2)} & 1-\frac{1}{2}\delta_1^{(1)}+\frac{3}{8}\delta_1^{(1)2}+\frac{3}{8}\delta_{81}^{(1)2}-\frac{1}{2}\delta_1^{(2)} \end{pmatrix}. \tag{34}$$

In terms of η_C, the Lagrangian reads

$$\mathcal{L}_C = \frac{1}{2}\partial_\mu \eta_C^T \partial^\mu \eta_C - \frac{1}{2}\eta_C^T \mathcal{M}_C^2 \eta_C, \tag{35}$$

with the mass matrix given by

$$\mathcal{M}_C^2 = \sqrt{Z}^T \mathcal{M}_B^2 \sqrt{Z} \equiv \begin{pmatrix} \hat{M}_8^2 & \hat{M}_{81}^2 \\ \hat{M}_{81}^2 & \hat{M}_1^2 \end{pmatrix}. \tag{36}$$

Up to and including second order in the corrections $\delta_j^{(i)}$ and $\Delta M_j^{2(i)}$, the entries of the matrix $\mathcal{M}_C^2$ read

$$\hat{M}_8^2 = \overset{\circ}{M}_8^2\left(1-\delta_8^{(1)}+\delta_8^{(1)2}+\frac{3}{4}\delta_{81}^{(1)2}-\delta_8^{(2)}\right) + \Delta M_8^{2(1)}(1-\delta_8^{(1)}) + \Delta M_8^{2(2)} + \overset{\circ}{M}_{81}^2\left(-\delta_{81}^{(1)}+\frac{3}{4}\delta_1^{(1)}\delta_{81}^{(1)}+\frac{5}{4}\delta_8^{(1)}\delta_{81}^{(1)}-\delta_{81}^{(2)}\right)$$
$$+ \Delta M_{81}^{2\,(1)}(-\delta_{81}^{(1)}) + \frac{1}{4}(M_0^2 + \overset{\circ}{M}_1^2)\delta_{81}^{(1)2}, \tag{37}$$

$$\hat{M}_1^2 = (M_0^2 + \overset{\circ}{M}_1^2)\left(1-\delta_1^{(1)}+\delta_1^{(1)2}+\frac{3}{4}\delta_{81}^{(1)2}-\delta_1^{(2)}\right) + \Delta M_1^{2(1)}(1-\delta_1^{(1)}) + \Delta M_1^{2(2)}$$
$$+ \overset{\circ}{M}_{81}^2\left(-\delta_{81}^{(1)}+\frac{3}{4}\delta_8^{(1)}\delta_{81}^{(1)}+\frac{5}{4}\delta_1^{(1)}\delta_{81}^{(1)}-\delta_{81}^{(2)}\right) + \Delta M_{81}^{2\,(1)}(-\delta_{81}^{(1)}) + \frac{1}{4}\overset{\circ}{M}_8^2\delta_{81}^{(1)2}, \tag{38}$$

$$\hat{M}_{81}^2 = \overset{\circ}{M}_{81}^2\left(1-\frac{1}{2}\delta_1^{(1)}-\frac{1}{2}\delta_8^{(1)}+\frac{3}{8}\delta_1^{(1)2}+\frac{1}{4}\delta_1^{(1)}\delta_8^{(1)}+\frac{3}{8}\delta_8^{(1)2}+\delta_{81}^{(1)2}-\frac{1}{2}\delta_1^{(2)}-\frac{1}{2}\delta_8^{(2)}\right)$$
$$+\Delta M_{81}^{2\,(1)}\left(1-\frac{1}{2}\delta_1^{(1)}-\frac{1}{2}\delta_8^{(1)}\right)+\Delta M_{81}^{2\,(2)}+\overset{\circ}{M}_8^2\left(-\frac{1}{2}\delta_{81}^{(1)}+\frac{3}{8}\delta_1^{(1)}\delta_{81}^{(1)}+\frac{5}{8}\delta_8^{(1)}\delta_{81}^{(1)}-\delta_{81}^{(2)}\right)+\Delta M_8^{2\,(1)}\left(-\frac{1}{2}\delta_{81}^{(1)}\right)$$
$$+(M_0^2+\overset{\circ}{M}_1^2)\left(-\frac{1}{2}\delta_{81}^{(1)}+\frac{3}{8}\delta_8^{(1)}\delta_{81}^{(1)}+\frac{5}{8}\delta_1^{(1)}\delta_{81}^{(1)}-\delta_{81}^{(2)}\right)+\Delta M_1^{2\,(1)}\left(-\frac{1}{2}\delta_{81}^{(1)}\right). \tag{39}$$

Finally, to obtain the physical mass eigenstates, we diagonalize the matrix $\mathcal{M}_C^2$ by means of an orthogonal transformation,

$$\eta_D = R\eta_C, \tag{40}$$
$$R \equiv \begin{pmatrix}\cos\theta^{[2]} & -\sin\theta^{[2]}\\ \sin\theta^{[2]} & \cos\theta^{[2]}\end{pmatrix}, \tag{41}$$

such that

$$R\mathcal{M}_C^2R^T = \mathcal{M}_D^2 = \begin{pmatrix}M_\eta^2 & 0\\ 0 & M_{\eta'}^2\end{pmatrix}. \tag{42}$$

The superscript [2] refers to corrections up to and including second order in the δ expansion. Introducing the nomenclature η_P for the physical fields and $\mathcal{M}_P^2$ for the diagonal mass matrix,

$$\eta_P = \eta_D = \begin{pmatrix}\eta\\ \eta'\end{pmatrix}, \qquad \mathcal{M}_P^2 = \begin{pmatrix}M_\eta^2 & 0\\ 0 & M_{\eta'}^2\end{pmatrix},$$

the Lagrangian is now of the free-field type,

$$\mathcal{L} = \mathcal{L}_D = \frac{1}{2}\partial_\mu\eta_P^T\partial^\mu\eta_P - \frac{1}{2}\eta_P^T\mathcal{M}_P^2\eta_P$$
$$= \frac{1}{2}\partial_\mu\eta\partial^\mu\eta - \frac{1}{2}M_\eta^2\eta^2 + \frac{1}{2}\partial_\mu\eta'\partial^\mu\eta' - \frac{1}{2}M_{\eta'}^2\eta'^2.$$

Equation (42) yields three relations,

$$\hat{M}_8^2 = M_\eta^2\cos^2\theta^{[2]} + M_{\eta'}^2\sin^2\theta^{[2]}, \tag{43}$$
$$\hat{M}_1^2 = M_\eta^2\sin^2\theta^{[2]} + M_{\eta'}^2\cos^2\theta^{[2]}, \tag{44}$$
$$\hat{M}_{81}^2 = (M_{\eta'}^2 - M_\eta^2)\sin\theta^{[2]}\cos\theta^{[2]}, \tag{45}$$

which *define* the mixing angle $\theta^{[2]}$ calculated up to and including $\mathcal{O}(\delta^2)$. First, from Eq. (45), we infer

$$\sin 2\theta^{[2]} = \frac{2\hat{M}_{81}^2}{M_{\eta'}^2 - M_\eta^2}. \tag{46}$$

Adding Eqs. (43) and (44), we obtain

$$M_{\eta'}^2 + M_\eta^2 = \hat{M}_8^2 + \hat{M}_1^2. \tag{47}$$

In the end, we subtract Eq. (44) from Eq. (43), take the square of the result, add the square of 2× Eq. (45), and take the square root of the result to obtain

$$M_{\eta'}^2 - M_\eta^2 = \sqrt{(\hat{M}_8^2 - \hat{M}_1^2)^2 + 4(\hat{M}_{81}^2)^2}. \tag{48}$$

This equation implies that Eq. (46) can also be written as

$$\sin 2\theta^{[2]} = \frac{2\hat{M}_{81}^2}{\sqrt{(\hat{M}_8^2 - \hat{M}_1^2)^2 + 4(\hat{M}_{81}^2)^2}}. \tag{49}$$

The transformation from the octet fields η_A to the physical fields η_D can be summarized as

$$\eta_A = T\eta_D = \left(1+\frac{1}{2}C_A\Box\right)\sqrt{Z}R^T\eta_D, \tag{50}$$

where the transformation matrix T is given by

$$T = \begin{pmatrix}-A\sin\theta^{[2]} + B_8\cos\theta^{[2]} & A\cos\theta^{[2]} + B_8\sin\theta^{[2]}\\ A\cos\theta^{[2]} - B_1\sin\theta^{[2]} & A\sin\theta^{[2]} + B_1\cos\theta^{[2]}\end{pmatrix}, \tag{51}$$

with

$$A = -\delta_{81}^{(1)}\left(\frac{1}{2}-\frac{3}{8}\delta_1^{(1)}-\frac{3}{8}\delta_8^{(1)}\right)-\frac{1}{2}\delta_{81}^{(2)}+\frac{c_{81}}{2}\Box, \tag{52}$$
$$B_i = 1-\frac{1}{2}\delta_i^{(1)}+\frac{3}{8}\delta_i^{(1)2}+\frac{3}{8}\delta_{81}^{(1)2}-\frac{1}{2}\delta_i^{(2)}+\frac{c_i}{2}\Box. \tag{53}$$

Up to this point, the procedure for defining a mixing angle in terms of successive transformations is rather general. We now turn to a determination of the quantities $\delta_i^{(j)}$ as well as the M_i^2 terms within $\mathrm{L}N_c\mathrm{ChPT}$. To identify $\mathcal{K}_A$ and $\mathcal{M}_A^2$ at NNLO, we calculate the self-energy insertions $-i\Sigma_{ij}(p^2)$, $(i,j=1,8)$ corresponding to the Feynman diagrams in Fig. 2. The Feynman rules are derived from the Lagrangians $\mathcal{L}^{(0)}$, $\mathcal{L}^{(1)}$, and $\mathcal{L}^{(2)}$ of Eqs. (9), (10), and (13)–(15). The self-energy calculated from the Lagrangian in Eq. (18) takes the form[9]

$$\Sigma(p^2) = \begin{pmatrix}\Sigma_{88}(p^2) & \Sigma_{81}(p^2)\\ \Sigma_{18}(p^2) & \Sigma_{11}(p^2)\end{pmatrix}, \tag{54}$$

[9]Since both the singlet and the octet states are massless in the combined chiral and $N_c\to\infty$ limits, we consider the lowest-order mass terms as part of the self-energy contributions.

where the $\Sigma_{ij}(p^2)$ are parametrized up to and including $\mathcal{O}(\delta^2)$ as

$$\Sigma_{88}(p^2) = -(k_8 + c_8 p^2)p^2 + M_8^2, \tag{55}$$

$$\Sigma_{81}(p^2) = \Sigma_{18}(p^2) = -(k_{81} + c_{81} p^2)p^2 + M_{81}^2, \tag{56}$$

$$\Sigma_{11}(p^2) = -(k_1 + c_1 p^2)p^2 + M_1^2. \tag{57}$$

We now obtain the elements of the kinematic matrix $\mathcal{K}_A$, the mass matrix $\mathcal{M}_A^2$, and the matrix $\mathcal{C}_A$ by comparing the results for the self-energies calculated by means of the Feynman diagrams (Fig. 2) with the parametrization given in Eqs. (55)–(57).

The NLO contributions to the kinetic matrix read

$$\delta_8^{(1)} = \frac{8(4M_K^2 - M_\pi^2)L_5}{3F_\pi^2}, \tag{58}$$

$$\delta_1^{(1)} = \frac{8(2M_K^2 + M_\pi^2)L_5}{3F_\pi^2} + \Lambda_1, \tag{59}$$

$$\delta_{81}^{(1)} = -\frac{16\sqrt{2}(M_K^2 - M_\pi^2)L_5}{3F_\pi^2}, \tag{60}$$

where M_π, M_K, and F_π denote the physical pion and kaon masses and the physical pion-decay constant, respectively. The difference between using physical values instead of leading-order expressions in Eqs. (58)–(60) is of NNLO and is compensated by an appropriate modification of the $\mathcal{O}(\delta^2)$ terms. The NNLO expressions for M_π, M_K, and F_π are displayed in Appendix B.

The entries of the mass matrix $\mathcal{M}_A^2$ are defined in Eqs. (29)–(31) in terms of leading-order, δ^1, and δ^2 pieces. The leading-order masses are given in Eqs. (22)–(25). In terms of the physical pion and kaon masses and the physical pion-decay constant, the first-order corrections read

$$\Delta M_8^{2(1)} = \frac{16(8M_K^4 - 8M_\pi^2 M_K^2 + 3M_\pi^4)L_8}{3F_\pi^2}, \tag{61}$$

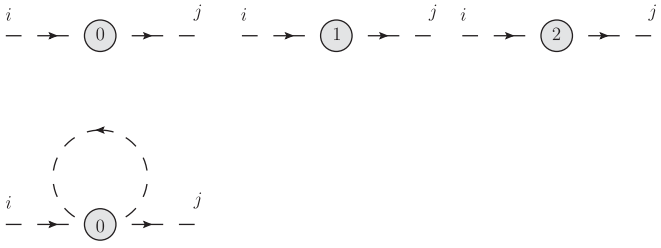

FIG. 2. Self-energy diagrams up to and including $\mathcal{O}(\delta^2)$: dashed lines refer to pseudoscalar mesons, and the numbers k in the interaction blobs refer to vertices derived from the corresponding Lagrangians $\mathcal{L}^{(k)}$.

$$\Delta M_1^{2(1)} = \frac{16(4M_K^4 - 4M_\pi^2 M_K^2 + 3M_\pi^4)L_8}{3F_\pi^2} + \frac{2\Lambda_2}{3}(2M_K^2 + M_\pi^2), \tag{62}$$

$$\Delta M_{81}^{2\,(1)} = -\frac{64\sqrt{2}(M_K^2 - M_\pi^2)M_K^2 L_8}{3F_\pi^2} - \frac{2\sqrt{2}\Lambda_2}{3}(M_K^2 - M_\pi^2). \tag{63}$$

The corresponding NNLO expressions for the kinetic and mass matrix elements can be found in Appendix C.

IV. DECAY CONSTANTS

The decay constants of the η-η' system are defined via the matrix element of the axial-vector-current operator $A_\mu^a = \bar{q}\gamma_\mu\gamma_5\frac{\lambda^a}{2}q$,

$$\langle 0|A_\mu^a(0)|P(p)\rangle = iF_P^a p_\mu, \tag{64}$$

where $a = 8, 0$ and $P = \eta, \eta'$. Since both mesons have octet and singlet components, Eq. (64) defines four independent decay constants, F_P^a. We parametrize them according to the convention in [36]

$$\{F_P^a\} = \begin{pmatrix} F_\eta^8 & F_\eta^0 \\ F_{\eta'}^8 & F_{\eta'}^0 \end{pmatrix} = \begin{pmatrix} F_8\cos\theta_8 & -F_0\sin\theta_0 \\ F_8\sin\theta_8 & F_0\cos\theta_0 \end{pmatrix}. \tag{65}$$

This parametrization is a popular way to define the η-η' mixing within the so-called two-angle scheme [45–52]. The angles θ_8 and θ_0 and the constants F_8 and F_0 are given by

$$\tan\theta_8 = \frac{F_{\eta'}^8}{F_\eta^8}, \qquad \tan\theta_0 = -\frac{F_\eta^0}{F_{\eta'}^0}, \tag{66}$$

$$F_8 = \sqrt{(F_\eta^8)^2 + (F_{\eta'}^8)^2}, \quad F_0 = \sqrt{(F_\eta^0)^2 + (F_{\eta'}^0)^2}. \tag{67}$$

To determine the decay constants F_P^a, we calculate the Feynman diagrams in Fig. 3. First, we calculate the coupling of the axial-vector current to the octet and singlet fields ϕ_b, collected in the doublet η_A, at the one-loop level up to NNLO in the δ counting. The result, which should be interpreted as a Feynman rule, is represented by the "matrix elements" $\mathcal{F}_{ab} = \langle 0|A_\mu^a(0)|b\rangle$. In a next step, we transform the bare fields η_A to the physical states using the transformation T in Eq. (51). The decay constants F_P^a are then given by

$$\{F_P^a\}^T = \begin{pmatrix} F_\eta^8 & F_\eta^0 \\ F_{\eta'}^8 & F_{\eta'}^0 \end{pmatrix}^T = (\mathcal{F}\cdot T). \tag{68}$$

At leading order, the decay constants read

$$F_\eta^8 = F_{\eta'}^0 = F\cos\theta^{[0]}, \tag{69}$$

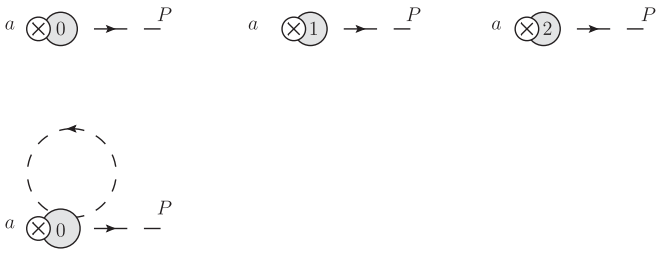

FIG. 3. Feynman diagrams contributing to the calculation of the decay constants up to and including $\mathcal{O}(\delta^2)$. Dashed lines refer to pseudoscalar mesons, crossed dots refer to axial-vector sources, and the numbers k in the interaction blobs refer to vertices derived from the Lagrangians $\mathcal{L}^{(k)}$ in Sec. II.

$$-F_\eta^0 = F_{\eta'}^8 = F\sin\theta^{[0]}, \tag{70}$$

in terms of the leading-order mixing angle $\theta^{[0]}$ given in Eq. (46). Equation (66) then yields $\theta_0 = \theta_8 = \theta^{[0]}$. The NLO decay constants are given by

$$F_\eta^8/F = \left(1+\frac{1}{2}\delta_8^{(1)}\right)\cos\theta^{[1]} - \frac{1}{2}\delta_{81}^{(1)}\sin\theta^{[1]}, \tag{71}$$

$$F_\eta^0/F = -\left(1+\frac{1}{2}\delta_1^{(1)}\right)\sin\theta^{[1]} + \frac{1}{2}\delta_{81}^{(1)}\cos\theta^{[1]}, \tag{72}$$

$$F_{\eta'}^8/F = \left(1+\frac{1}{2}\delta_8^{(1)}\right)\sin\theta^{[1]} + \frac{1}{2}\delta_{81}^{(1)}\cos\theta^{[1]}, \tag{73}$$

$$F_{\eta'}^0/F = \left(1+\frac{1}{2}\delta_1^{(1)}\right)\cos\theta^{[1]} + \frac{1}{2}\delta_{81}^{(1)}\sin\theta^{[1]}, \tag{74}$$

now in terms of the NLO mixing angle $\theta^{[1]}$. Using Eqs. (66) and (67), one obtains

$$F_8 = F\left(1+\frac{\delta_8^{(1)}}{2}\right),$$
$$F_0 = F\left(1+\frac{\delta_1^{(1)}}{2}\right), \tag{75}$$

and

$$\theta_8 = \theta^{[1]} + \arctan\left(\frac{\delta_{81}^{(1)}}{2}\right),$$
$$\theta_0 = \theta^{[1]} - \arctan\left(\frac{\delta_{81}^{(1)}}{2}\right). \tag{76}$$

The results for the decay constants at NNLO are lengthy and are given in Appendix B.

V. NUMERICAL ANALYSIS

In the following, we perform the numerical evaluation of the mixing angle, the masses of the pseudoscalar mesons, and their decay constants. We present the results in a systematic way, order by order.

A. Leading order

At leading order (LO), the mixing angle is given by Eq. (49), which reduces to

$$\sin 2\theta^{[0]} = \frac{-4\sqrt{2}(M_K^2 - M_\pi^2)}{\sqrt{12M_0^2(M_\pi^2 - M_K^2) + 36(M_K^2 - M_\pi^2)^2 + 9M_0^4}}. \tag{77}$$

This equation is well suited to study the two limits, the flavor-symmetric case, i.e., $M_\pi^2 = M_K^2$, and the limit $N_c \to \infty$. In the flavor-symmetric limit, the mixing angle vanishes, $\theta^{[0]} = 0$. On the other hand, in the LN_c limit, the U(1)$_A$ contribution to the η' mass vanishes, i.e., $M_0^2 = 0$, and the mixing angle becomes independent of the pseudoscalar masses

$$\sin 2\theta^{[0]} = -\frac{2\sqrt{2}}{3}, \tag{78}$$

which yields $\theta^{[0]} = -35.3°$. We then turn to the physical case. Employing Eqs. (47) and (48), we fix M_0^2 to the physical $M_{\eta'}^2$ mass

$$M_0^2 = \frac{3(M_{\eta'}^2 - M_\pi^2)(2M_K^2 - M_{\eta'}^2 - M_\pi^2)}{4M_K^2 - 3M_{\eta'}^2 - M_\pi^2} \tag{79}$$

and obtain

$$\sin 2\theta^{[0]} = -\frac{4\sqrt{2}(M_K^2 - M_\pi^2)(-4M_K^2 + 3M_{\eta'}^2 + M_\pi^2)}{3[-8M_K^2(M_{\eta'}^2 + M_\pi^2) + 8M_K^4 + 3M_{\eta'}^4 + 2M_\pi^2 M_{\eta'}^2 + 3M_\pi^4]}. \tag{80}$$

Evaluating these results for physical masses M_π^2, M_K^2, and $M_{\eta'}^2$ yields

$$\theta^{[0]} = -19.6° \quad \text{and} \quad M_0 = 0.820\ \text{GeV}. \tag{81}$$

B. NLO

At NLO, still only tree diagrams contribute, since loop contributions are relegated to NNLO. Beyond F, $B\hat{m}$, Bm_s, and τ, the four NLO LECs L_5, L_8, Λ_1, and Λ_2 appear and need to be fixed. Since there are, at present, no values for all of the NLO LECs in U(3) ChPT available in the literature, we follow two different strategies to fix the coupling constants:

(1) We design a compact system of observables calculated within our framework of LN_cChPT and determine the LECs by fixing them to the physical values of the observables. Our set of observables consists of M_π^2, M_K^2, F_K/F_π, M_η^2, and $M_{\eta'}^2$. In addition, we need the quark-mass ratio $m_s/\hat{m}$, which we take from Ref. [67]. The experimental values for the masses and decay constants are taken from Ref. [1], reading

$$M_\pi = 0.135\ \text{GeV}, \qquad M_K = 0.494\ \text{GeV},$$
$$M_\eta = 0.548\ \text{GeV},$$
$$M_{\eta'} = 0.958\ \text{GeV}, \qquad F_\pi = 0.0922(1)\ \text{GeV},$$
$$F_K/F_\pi = 1.198(6). \tag{82}$$

(2) We use phenomenological determinations of some constants obtained in SU(3) ChPT, for example, Table 1 from Ref. [44].

We start with the first strategy and begin by fixing M_0^2 to the physical $M_{\eta'}^2$ using the relation

$$(2M_{\eta'}^2 - \hat{M}_8^2 - \hat{M}_1^2)^2 = (\hat{M}_8^2 - \hat{M}_1^2)^2 + 4(\hat{M}_{81}^2)^2, \tag{83}$$

which follows from Eqs. (47) and (48). After expressing M_0^2 in terms of $M_{\eta'}^2$, the parameters Λ_1 and Λ_2 appear only in the QCD-scale-invariant combination $\tilde{\Lambda} = \Lambda_1 - 2\Lambda_2$ [35] in the expressions for our observables and the mixing angle. Using the ratio $m_s/\hat{m} = 27.5$ from Ref. [67], the parameters $B\hat{m}$, L_5, L_8, and $\tilde{\Lambda}$ can be unambiguously obtained from the NLO relations for the physical values of M_π^2, M_K^2, F_K/F_π, and M_η^2, given in Appendix B. The results for the LECs are shown in Table II, labeled NLO I. Notice that at this order no EFT-scale dependence is introduced yet, so these LECs are scale independent. We also display errors for all calculated quantities. These errors are only due to the input errors. We do not give estimates for the errors due to neglecting higher orders or particular assumptions of our models. As input errors, we consider the errors of F_K/F_π, F_π, and $m_s/\hat{m}$, and, later, when we make use of LECs determined in SU(3) ChPT [44], we also take their errors into account.

Once the set of LECs is determined, we can evaluate the LO pseudoscalar masses, the η-η' mixing angle, and the pseudoscalar decay constants. For the calculation of the parameters θ_8, θ_0, F_8, and F_0, we use the simplified formula at NLO given in Eqs. (75) and (76). The quantities M_0^2 and F_0 depend on the QCD-renormalization scale [35]. Therefore, we can only provide the QCD-scale-invariant quantities $M_0^2/(1+\Lambda_1)$ and $F_0/(1+\Lambda_1/2)$. We are not able to extract a value for Λ_1 from our observables, since physical observables do not depend on the QCD scale and we can only determine the invariant combination $\tilde{\Lambda} = \Lambda_1 - 2\Lambda_2$. The expressions for $M_0^2/(1+\Lambda_1)$ and $F_0/(1+\Lambda_1/2)$ are expanded up to NLO, yielding results which depend on Λ_1 only through $\tilde{\Lambda}$. Table III shows the leading-order masses $\overset{\circ}{M}_\pi^2$, $\overset{\circ}{M}_K^2$, $M_0^2/(1+\Lambda_1)$, and M_η^2 for $\tilde{\Lambda} = 0$. The mixing angle $\theta^{[1]}$, the angles θ_8 and θ_0, and the constants F_8 and $F_0/(1+\Lambda_1/2)$ are shown in Table IV, again under the label NLO I.

The second scenario uses values for the LECs determined phenomenologically in the framework of SU(3) ChPT. Since our calculations are performed in U(3) ChPT, we apply the appropriate matching between the two EFTs [35,38] when we make use of SU(3) determinations. We set the matching scale of the two theories to be $\mu_0 = M_0 = 0.85$ GeV, which is basically the value of $M_{\eta'}$ in the chiral limit: $M_0^2 = 6\tau/(F^2(1+\Lambda_1))$. Since SU(3) ChPT contains one-loop corrections already at NLO, the LECs depend on the scale of the effective theory μ. The SU(3) LECs are typically provided at $\mu_1 = 0.77$ GeV. To study the scale dependence of our results, we evaluate them at $\mu = 0.77$ GeV and at $\mu = 1$ GeV, which is the scale of $M_{\eta'}$. Combining the matching at μ_0 and the running from μ_1 to μ results in [35,38]

TABLE II. LECs at NLO.

	μ (GeV)	L_5 $[10^{-3}]$	L_8 $[10^{-3}]$	$\tilde{\Lambda}$
NLO I	⋯	1.86 ± 0.06	0.78 ± 0.05	-0.34 ± 0.05
NLO II	0.77	1.20 ± 0.10	0.55 ± 0.20	0.02 ± 0.13
NLO II	1	0.58 ± 0.10	0.24 ± 0.20	0.41 ± 0.13

TABLE III. Pseudoscalar masses at NLO in GeV^2.

	μ (GeV)	$\overset{\circ}{M}_\pi^2$	$\overset{\circ}{M}_K^2$	$\frac{M_0^2}{(1+\Lambda_1)}$	$M_\eta^2(\tilde{\Lambda}=0)$
NLO I	⋯	0.018 ± 0.000	0.261 ± 0.005	0.902 ± 0.013	0.326 ± 0.003
NLO II	0.77	0.018 ± 0.000	0.249 ± 0.023	0.871 ± 0.061	0.299 ± 0.010
NLO II	1	0.018 ± 0.000	0.249 ± 0.023	0.871 ± 0.061	0.269 ± 0.010

TABLE IV. Mixing angles and decay constants at NLO.

	μ (GeV)	θ (°)	θ_8 (°)	θ_0 (°)	F_8/F_π	$\frac{F_0}{1+\Lambda_1/2}/F_\pi$
NLO I	⋯	-11.1 ± 0.6	-21.7 ± 0.7	-0.5 ± 0.7	1.26 ± 0.01	1.13 ± 0.00
NLO II	0.77	-12.6 ± 3.0	-19.5 ± 3.0	-5.7 ± 3.2	1.17 ± 0.01	1.09 ± 0.01
NLO II	1	-12.6 ± 3.0	-15.9 ± 3.0	-9.3 ± 3.2	1.08 ± 0.01	1.04 ± 0.01

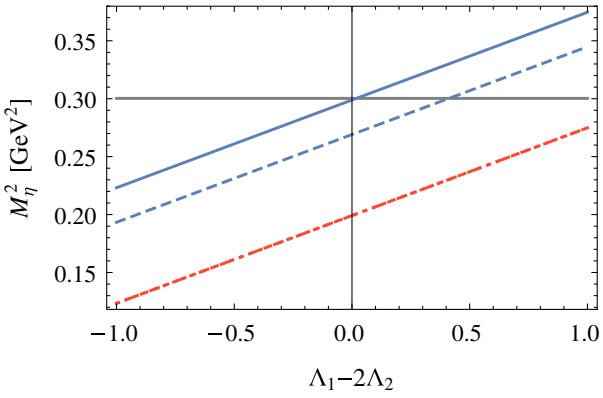

FIG. 4. M_η^2 as a function of $\tilde{\Lambda} = \Lambda_1 - 2\Lambda_2$. Solid (blue) line: NLO II at 0.77 GeV; dashed (blue) line: NLO II at 1 GeV. Dotted-dashed (red) line: NLO + loops II at 0.77 GeV; dotted (red) line: NLO + loops II at 1 GeV. The dotted-dashed and dotted lines coincide. Horizontal line: physical value.

$$
\begin{aligned}
L_5^r(\mu) &= L_5^{\mathrm{SU}_3,r}(\mu_1) + \frac{3}{8}\frac{1}{16\pi^2}\ln\left(\frac{\mu_1}{\mu}\right),\\
L_8^r(\mu) &= L_8^{\mathrm{SU}_3,r}(\mu_1) + \frac{5}{48}\frac{1}{16\pi^2}\ln\left(\frac{\mu_1}{\mu}\right) + \frac{1}{12}\frac{1}{16\pi^2}\ln\left(\frac{\mu_0}{\mu}\right),\\
L_4^r(\mu) &= L_4^{\mathrm{SU}_3,r}(\mu_1) + \frac{1}{8}\frac{1}{16\pi^2}\ln\left(\frac{\mu_1}{\mu}\right),\\
L_6^r(\mu) &= L_6^{\mathrm{SU}_3,r}(\mu_1) + \frac{11}{144}\frac{1}{16\pi^2}\ln\left(\frac{\mu_1}{\mu}\right)\\
&\quad + \frac{1}{72}\frac{1}{16\pi^2}\left(\frac{1}{2} - \ln\left(\frac{\mu_0}{\mu}\right)\right),\\
L_7^r(\mu) &= L_7^{\mathrm{SU}_3,r} + \frac{F^4(1+\Lambda_2)^2}{288\tau},\\
L_{18}^r(\mu) &= L_{18}^r(\mu_2) - \frac{1}{4}\frac{1}{16\pi^2}\ln\left(\frac{\mu_2}{\mu}\right).
\end{aligned}
\tag{84}
$$

The constant L_{18} does not appear in SU(3) ChPT, but we include its running for completeness, since the running from the scale $\mu_2 = 1$ GeV will be needed later.

The LO quantities $\overset{\circ}{M}{}_\pi^2$, $\overset{\circ}{M}{}_K^2$, and F are expressed in terms of the physical quantities M_π^2, M_K^2, and F_π, and, again, M_0^2 is determined from the relation to $M_{\eta'}^2$ at this order. The parameters θ_8, θ_0, F_8, and F_0 are calculated using Eqs. (75) and (76). For the LECs L_5 and L_8, we use the values determined at $\mathcal{O}(p^4)$ in SU(3) ChPT, i.e., column "p^4 fit" in Table 1 in Ref. [44]. The OZI rule-violating parameter $\tilde{\Lambda}$ is fixed to M_η^2. The results are given in Tables II–IV, labeled NLO II. The dependence of M_η^2 on $\tilde{\Lambda}$ is shown in Fig. 4.

C. NLO + loops

Before considering the full NNLO corrections, we first discuss the case where we just add the loop contributions to the NLO expressions. Since the loop corrections do not contain any unknown parameters, we can use exactly the same system of equations from the NLO I scenario in the previous section to obtain the desired LECs. We augment the system of linear equations with the one-loop corrections and extract the values of $B\hat{m}$, L_5, L_8, and $\tilde{\Lambda}$. The results depend now on the scale of the effective theory, and we choose to extract the LECs at $\mu = 1$ GeV. The parameters θ_8, θ_0, F_8, and F_0 are obtained from Eqs. (B10)–(B13) in Appendix B, now also including the one-loop corrections. The results are given in Tables V–VII, labeled NLO + loops I.

We compare the results with the values obtained in SU(3) ChPT. For L_5 and L_8, we use the same values as in the NLO II case. To compensate the scale dependence of the loop contributions, we include the scale-dependent parts of the LECs L_4, L_6, L_7, and L_{18} [see Eqs. (84)], which would appear only at NNLO. These constants are included

TABLE V. LECs at NLO with loops added.

	μ (GeV)	L_5 $[10^{-3}]$	L_8 $[10^{-3}]$	$\tilde{\Lambda}$
NLO + loops I	0.77	1.37 ± 0.06	0.85 ± 0.05	0.52 ± 0.05
NLO + loops I	1	0.75 ± 0.06	0.55 ± 0.05	1.09 ± 0.04
NLO + loops II	0.77	1.20 ± 0.10	0.55 ± 0.20	1.34 ± 0.13
NLO + loops II	1	0.58 ± 0.10	0.24 ± 0.20	1.34 ± 0.13

TABLE VI. Pseudoscalar masses at NLO with loops added in GeV^2.

	μ (GeV)	$\overset{\circ}{M}{}_\pi^2$	$\overset{\circ}{M}{}_K^2$	$\frac{M_0^2}{(1+\Lambda_1)}$	$M_\eta^2(\tilde{\Lambda}=0)$
NLO + loops I	0.77	0.018 ± 0.000	0.263 ± 0.005	0.927 ± 0.013	0.261 ± 0.003
NLO + loops I	1	0.017 ± 0.000	0.240 ± 0.005	0.867 ± 0.012	0.218 ± 0.003
NLO + loops II	0.77	0.019 ± 0.000	0.287 ± 0.023	0.933 ± 0.061	0.199 ± 0.010
NLO + loops II	1	0.017 ± 0.000	0.265 ± 0.023	0.933 ± 0.061	0.199 ± 0.010

TABLE VII. Mixing angles and decay constants at NLO with loops added.

	μ (GeV)	θ (°)	θ_8 (°)	θ_0 (°)	F_8/F_π	$\frac{F_0}{1+\Lambda_1/2}/F_\pi$
NLO + loops I	0.77	-10.2 ± 0.6	-18.0 ± 0.7	-2.4 ± 0.7	1.31 ± 0.01	0.97 ± 0.00
NLO + loops I	1	-13.4 ± 0.6	-17.7 ± 0.7	-9.1 ± 0.7	1.31 ± 0.01	0.87 ± 0.00
NLO + loops II	0.77	-10.2 ± 2.9	-13.5 ± 2.9	-6.8 ± 3.1	1.28 ± 0.01	0.86 ± 0.01
NLO + loops II	1	-10.2 ± 2.9	-13.5 ± 2.9	-6.8 ± 3.1	1.28 ± 0.01	0.86 ± 0.01

without the SU(3)-U(3) matching, and we choose $L_4^r = L_6^r = L_7^r = L_{18}^r = 0$ at $\mu_1 = 1$ GeV. Eventually, we again use M_η^2 to extract $\tilde{\Lambda}$. Equations (B10)–(B13) in Appendix B provide then our values for θ_8, θ_0, F_8, and F_0. The results can be found in Tables V–VII, denoted by NLO + loops II. Figure 4 shows the dependence of M_η^2 on $\tilde{\Lambda}$ for the different scenarios discussed so far. We notice that the dependence is quite strong. After the inclusion of the loops and the scale-dependent parts of the $1/N_c$-suppressed L_i, M_η^2 is independent of the renormalization scale μ (dotted and dotted-dashed red lines).

D. NNLO

At NNLO, there are too many unknown LECs, which cannot be determined from our chosen set of observables. This means that it is not possible to consistently determine all LECs appearing at NNLO within our framework of LN_cChPT. So, we can only employ the second strategy and make use of phenomenological determinations of the LECs L_i and C_i in SU(3) ChPT. We are then left with five completely unknown LECs, Λ_1, Λ_2, L_{18}, L_{25}, and $v_2^{(2)}$, and the combination $L_{46} + L_{53}$, which are related to the singlet field. First, we investigate the case with $C_i = 0$. We match the L_i from SU(3) to U(3), according to Eq. (84), and take their values from the column p^4 fit in Table 1 in Ref. [44]. Since a NNLO calculation in the δ counting includes contributions of the type NLO × NLO, e.g., products of L_i, the results depend on the EFT scale μ. We display results for two different scales, $\mu = 0.77$ GeV and $\mu = 1$ GeV. We choose $\Lambda_1 = \Lambda_2 = L_{18}^r = v_2^{(2)} = L_{46} = L_{53} = 0$ at $\mu_2 = 1$ GeV, which, together with the U(3)-SU(3) matching, results in $L_7^r \approx 0$ (at $\mu = 1$ GeV). We can then fix one OZI rule-violating LEC, which we choose to be L_{25}, to the physical value of M_η^2. In this way, L_{25} accounts for the contributions to M_η^2 of all other OZI rule-violating LECs, which are put to zero. At NNLO including C_{12} terms, the simplified expressions for θ_8, θ_0, F_8, and F_0 in Eqs. (75) and (76) no longer hold. We therefore use the general formulas in Eqs. (66) and (67) to calculate the parameters of the two-angle scheme in the NNLO scenarios. The results are given in Tables VIII–X, labeled NNLO w/o Ci. Figure 5 shows M_η^2 as a function of L_{25}.

Finally, we include the contributions of the C_i. The L_i are treated as before in terms of running and matching, but now we use the $\mathcal{O}(p^6)$ values from Ref. [44], i.e., column "BE14" in Table 3. For the C_i, we employ the values from Table 4 in Ref. [44]. In order to obtain values for the C_i in U(3) ChPT, we employ the tree-level matching relations between SU(3) and U(3) ChPT, given by [68]

$$C_{19} = C_{19}^{\mathrm{SU}_3} + \frac{1}{3}\frac{F^2}{48M_0^4},$$
$$C_{31} = C_{31}^{\mathrm{SU}_3} + \frac{F^2}{48M_0^4}, \tag{85}$$

where we take $F = F_\pi$ and the LO value $M_0^2 = 0.673\ \mathrm{GeV}^2$. We do not consider the matching at the loop level, because this is a correction beyond the accuracy of our calculation. We also do not include the dependence of the C_i on the EFT-renormalization scale, since this would be introduced only by two-loop effects, which are again higher-order contributions beyond our accuracy. The SU(3) values of the C_i are provided without errors. They are also not very well constrained in Ref. [44] and might be only suited for the SU(3) observables studied in this reference. Therefore, we assume an error of 50% on the SU(3) values and propagate it to our results. The dependence of M_η^2 on L_{25} is shown in Fig. 5, and eventually L_{25} is fixed to the physical value of M_η^2. The results are given in Tables VIII–X, labeled NNLO w/ Ci.

Another source for the L_i and C_i is provided in Ref. [69], where the LECs are computed in a chiral quark model.

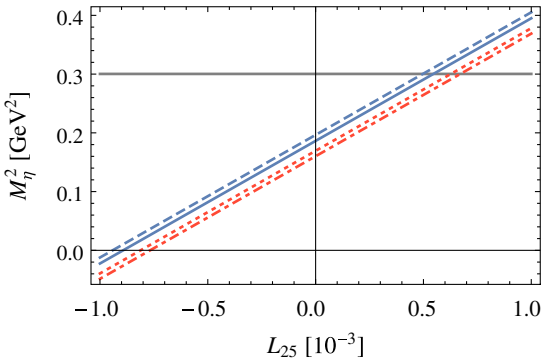

FIG. 5. M_η^2 as a function of L_{25}. Solid (blue) line: NNLO without C_i at 0.77 GeV; dashed (blue) line: NNLO without C_i at 1 GeV. Dotted-dashed (red) line: NNLO with C_i at 0.77 GeV; dotted (red) line: NNLO with C_i at 1 GeV. Horizontal line: physical value.

TABLE VIII. LECs at NNLO.

	μ (GeV)	L_5 $[10^{-3}]$	L_8 $[10^{-3}]$	L_{25} $[10^{-3}]$
NNLO w/o Ci	0.77	1.20 ± 0.10	0.55 ± 0.20	0.55 ± 0.08
NNLO w/o Ci	1	0.58 ± 0.10	0.24 ± 0.20	0.50 ± 0.08
NNLO w/ Ci	0.77	1.01 ± 0.06	0.52 ± 0.10	0.67 ± 0.13
NNLO w/ Ci	1	0.39 ± 0.06	0.21 ± 0.10	0.63 ± 0.13
NNLO w/ Ci J	0.77	1.26 ± 0.06	0.84 ± 0.05	0.70 ± 0.07
NNLO w/ Ci J	1	1.26 ± 0.06	0.84 ± 0.05	0.77 ± 0.07

TABLE IX. Pseudoscalar masses at NNLO in GeV^2.

	μ (GeV)	$\mathring{M}_\pi^2$	$\mathring{M}_K^2$	$\frac{M_0^2}{(1+\Lambda_1)}$	$M_\eta^2(L_{25}=0)$
NNLO w/o Ci	0.77	0.018 ± 0.007	0.277 ± 0.101	0.840 ± 0.154	0.186 ± 0.016
NNLO w/o Ci	1	0.016 ± 0.007	0.257 ± 0.102	0.841 ± 0.158	0.197 ± 0.017
NNLO w/ Ci	0.77	0.018 ± 0.001	0.267 ± 0.040	0.521 ± 0.170	0.160 ± 0.028
NNLO w/ Ci	1	0.017 ± 0.001	0.246 ± 0.041	0.518 ± 0.171	0.169 ± 0.028
NNLO w/ Ci J	0.77	0.018 ± 0.000	0.232 ± 0.024	0.729 ± 0.088	0.153 ± 0.014
NNLO w/ Ci J	1	0.017 ± 0.000	0.210 ± 0.024	0.670 ± 0.088	0.140 ± 0.014

TABLE X. Mixing angles and decay constants at NNLO.

	μ (GeV)	θ (°)	θ_8 (°)	θ_0 (°)	F_8/F_π	$\frac{F_0}{1+\Lambda_1/2}/F_\pi$
NNLO w/o Ci	0.77	-9.6 ± 6.0	-11.7 ± 5.8	-6.6 ± 6.4	1.27 ± 0.02	0.85 ± 0.01
NNLO w/o Ci	1	-10.1 ± 6.3	-12.6 ± 6.1	-6.3 ± 6.5	1.28 ± 0.02	0.86 ± 0.01
NNLO w/ Ci	0.77	-33.8 ± 18.8	-31.8 ± 18.5	-32.4 ± 21.1	1.17 ± 0.07	0.82 ± 0.01
NNLO w/ Ci	1	-35.2 ± 21.5	-33.7 ± 21.5	-33.3 ± 24.2	1.18 ± 0.08	0.83 ± 0.01
NNLO w/ Ci J	0.77	-16.8 ± 4.9	-16.0 ± 4.4	-11.7 ± 6.1	1.16 ± 0.04	0.90 ± 0.02
NNLO w/ Ci J	1	-20.2 ± 5.4	-19.4 ± 4.9	-15.3 ± 6.7	1.24 ± 0.04	0.84 ± 0.02

Since the LECs are calculated in the LN_c limit, loop effects are not included, and the LECs do not depend on the EFT-renormalization scale. Thus, to obtain values for the LECs in U(3) ChPT, we consider only the tree-level SU(3)-U(3) matching relations (for L_7, C_{19}, and C_{31}). Further, we do not take the running of the LECs with the EFT scale into account. The one-loop contributions are evaluated at $\mu = 0.77$ GeV and $\mu = 1$ GeV. The OZI rule-violating couplings are treated as in the other NNLO scenarios described above. The results are provided in Tables VIII–X, labeled NNLO w/ Ci J, where the errors are obtained from the errors of the L_i and C_i given in Ref. [69].

Figure 5 shows a strong dependence of M_η^2 on L_{25}. The renormalization-scale dependence is now much smaller than in the NLO cases. The small residual scale dependence stems from products of L_5 and L_8, the scale dependence of which would be compensated by products of one-loop terms in the full two-loop calculation. The inclusion of the one-loop corrections decreases the value of $M_\eta^2(L_{25}=0)$ by about 30%. This would rather match the expected order of magnitude of a NLO correction. Taking the C_i into account further decreases $M_\eta^2(L_{25}=0)$. According to the δ counting, we would expect the value for L_{25} to be of the same order of magnitude as L_5 and L_8, since the operator structure is similar, with an additional $1/N_c$ suppression leading to $|L_{25}| \sim \frac{1}{3} \times 10^{-3}$. The fit to the physical M_η^2 results in values for L_{25} which match this expectation pretty well.

E. Discussion of the results

In the following, we discuss the summaries of our results in Tables XI–XIII. A summary of the LECs used in the different scenarios is provided in Tables XIV–XVI in Appendix D. We start with the results for the masses summarized in Table XI. The values for the squared pion mass at LO are very close to the physical squared pion mass with deviations of 10%. The LO squared kaon masses are larger than the physical value, up to about 25%, except for the NNLO w/ Ci J scenario. The positive NLO and NNLO corrections are in accordance with the findings in Ref. [44]. The LO squared pion and kaon masses, $2\hat{m}B$ and $(\hat{m}+m_s)B$, respectively, show a renormalization-scale dependence, which is caused by the renormalization of the parameter B in U(3) ChPT. The squared singlet mass in the chiral limit, $M_0^2/(1+\Lambda_1)$, increases by about 30% in most of the higher-order scenarios compared to the LO

TABLE XI. Summary of the results for the pseudoscalar masses in GeV^2. The parameter x denotes $\tilde{\Lambda}$ or L_{25}.

	μ (GeV)	$\overset{\circ}{M}{}^2_\pi$	$\overset{\circ}{M}{}^2_K$	$\frac{M_0^2}{(1+\Lambda_1)}$	$M^2_\eta(x=0)$
LO	⋯	0.018 ± 0	0.244 ± 0	0.673 ± 0	0.244 ± 0
NLO I	⋯	0.018 ± 0.000	0.261 ± 0.005	0.902 ± 0.013	0.326 ± 0.003
NLO + loops I	0.77	0.018 ± 0.000	0.263 ± 0.005	0.927 ± 0.013	0.261 ± 0.003
NLO + loops I	1	0.017 ± 0.000	0.240 ± 0.005	0.867 ± 0.012	0.218 ± 0.003
NLO II	0.77	0.018 ± 0.000	0.249 ± 0.023	0.871 ± 0.061	0.299 ± 0.010
NLO II	1	0.018 ± 0.000	0.249 ± 0.023	0.871 ± 0.061	0.269 ± 0.010
NLO + loops II	0.77	0.019 ± 0.000	0.287 ± 0.023	0.933 ± 0.061	0.199 ± 0.010
NLO + loops II	1	0.017 ± 0.000	0.265 ± 0.023	0.933 ± 0.061	0.199 ± 0.010
NNLO w/o Ci	0.77	0.018 ± 0.007	0.277 ± 0.101	0.840 ± 0.154	0.186 ± 0.016
NNLO w/o Ci	1	0.016 ± 0.007	0.257 ± 0.102	0.841 ± 0.158	0.197 ± 0.017
NNLO w/ Ci	0.77	0.018 ± 0.001	0.267 ± 0.040	0.521 ± 0.170	0.160 ± 0.028
NNLO w/ Ci	1	0.017 ± 0.001	0.246 ± 0.041	0.518 ± 0.171	0.169 ± 0.028
NNLO w/ Ci J	0.77	0.018 ± 0.000	0.232 ± 0.024	0.729 ± 0.088	0.153 ± 0.014
NNLO w/ Ci J	1	0.017 ± 0.000	0.210 ± 0.024	0.670 ± 0.088	0.140 ± 0.014

TABLE XII. Summary of the results for the mixing angles.

	μ (GeV)	θ (°)	θ_8 (°)	θ_0 (°)
LO	⋯	-19.6 ± 0	-19.6 ± 0	-19.6 ± 0
NLO I	⋯	-11.1 ± 0.6	-21.7 ± 0.7	-0.5 ± 0.7
NLO + loops I	0.77	-10.2 ± 0.6	-18.0 ± 0.7	-2.4 ± 0.7
NLO + loops I	1	-13.4 ± 0.6	-17.7 ± 0.7	-9.1 ± 0.7
NLO II	0.77	-12.6 ± 3.0	-19.5 ± 3.0	-5.7 ± 3.2
NLO II	1	-12.6 ± 3.0	-15.9 ± 3.0	-9.3 ± 3.2
NLO + loops II	0.77	-10.2 ± 2.9	-13.5 ± 2.9	-6.8 ± 3.1
NLO + loops II	1	-10.2 ± 2.9	-13.5 ± 2.9	-6.8 ± 3.1
NNLO w/o Ci	0.77	-9.6 ± 6.0	-11.7 ± 5.8	-6.6 ± 6.4
NNLO w/o Ci	1	-10.1 ± 6.3	-12.6 ± 6.1	-6.3 ± 6.5
NNLO w/ Ci	0.77	-33.8 ± 18.8	-31.8 ± 18.5	-32.4 ± 21.1
NNLO w/ Ci	1	-35.2 ± 21.5	-33.7 ± 21.5	-33.3 ± 24.2
NNLO w/ Ci J	0.77	-16.8 ± 4.9	-16.0 ± 4.4	-11.7 ± 6.1
NNLO w/ Ci J	1	-20.2 ± 5.4	-19.4 ± 4.9	15.3 ± 6.7

TABLE XIII. Summary of the results for the decay constants.

	μ (GeV)	F_8/F_π	$\frac{F_0}{1+\Lambda_1/2}/F_\pi$	F (MeV)
LO	⋯	1 ± 0	1 ± 0	92.2 ± 0.1
NLO I	⋯	1.26 ± 0.01	1.13 ± 0.00	90.73 ± 0.11
NLO + loops I	0.77	1.31 ± 0.01	0.97 ± 0.00	79.31 ± 0.12
NLO + loops I	1	1.31 ± 0.01	0.87 ± 0.00	74.77 ± 0.12
NLO II	0.77	1.17 ± 0.01	1.09 ± 0.01	91.25 ± 0.13
NLO II	1	1.08 ± 0.01	1.04 ± 0.01	91.74 ± 0.13
NLO + loops II	0.77	1.28 ± 0.01	0.86 ± 0.01	74.91 ± 0.14
NLO + loops II	1	1.28 ± 0.01	0.86 ± 0.01	74.91 ± 0.14
NNLO w/o Ci	0.77	1.27 ± 0.02	0.85 ± 0.01	79.46 ± 6.59
NNLO w/o Ci	1	1.28 ± 0.02	0.86 ± 0.01	79.45 ± 6.59
NNLO w/ Ci	0.77	1.17 ± 0.07	0.82 ± 0.01	73.02 ± 0.13
NNLO w/ Ci	1	1.18 ± 0.08	0.83 ± 0.01	73.02 ± 0.13
NNLO w/ Ci J	0.77	1.16 ± 0.04	0.90 ± 0.02	79.44 ± 0.12
NNLO w/ Ci J	1	1.24 ± 0.04	0.84 ± 0.02	74.40 ± 0.13

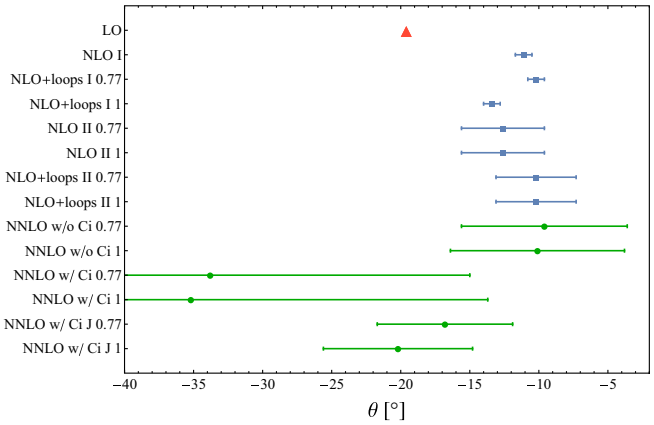

FIG. 6. Results for the mixing angle θ obtained within the different scenarios in this work.

value, except for the NNLO w/ Ci case, where we can see a strong influence of the C_i contributions. However, a direct comparison to the LO value, M_0^2, remains difficult, since we do not know the value of Λ_1. The column $M_\eta^2(x=0)$ shows the value of M_η^2 if the OZI rule-violating parameter $\tilde{\Lambda}$ or L_{25}, which is fixed to the physical M_η^2, is switched off. Especially in the NNLO scenarios, the resulting values are only 50% of the physical M_η^2. Therefore, we conclude that employing the LECs determined in SU(3) ChPT is not sufficient in a LN_cChPT calculation and OZI rule-violating couplings need to be included to adequately describe M_η^2. The same conclusion applies to the NNLO w/ Ci J case. The contributions of the OZI rule-violating parameters $\tilde{\Lambda}$ and L_{25} are very important. One should also keep in mind that we only retained L_{25} and omitted all other OZI rule-violating LECs in the NNLO cases.

A summary of the results for the mixing angle θ is shown in Fig. 6. In comparison to the LO value $\theta = -19.6°$, in the cases without C_i, θ gets shifted to values between $-9°$ and $-14°$. The results of the NNLO w/ Ci J scenario are close to the LO value. Including the C_i obtained in SU(3) ChPT (NNLO w/ Ci) leads to a drastic change of θ, where the large errors are mainly caused by the assumed 50% errors of the input C_i. The mixing angle seems to be very sensitive to the values of the C_i, although they are supposed to give only small contributions since they are NNLO corrections. We display the results for the angles θ_8 and θ_0 and the constants F_8 and F_0 in Figs. 7 and 8, respectively. They are compared to other phenomenological determinations. Reference [36] determined the mixing parameters at NLO in LN_cChPT using additional input from the two-photon decays of η and η'. References [45,47,48,51,52] employed the two-angle scheme to extract the mixing parameters phenomenologically from decays involving η and η', mostly the two-photon decays, but other processes, e.g., $\eta^{(\prime)}V\gamma$ with vector mesons V, were used as well [47]. Note, however, these other determinations were performed only in a NLO framework and under certain assumptions, e.g., neglecting OZI rule-violating couplings [45]. A study of the η-η' mixing at NNLO in LN_cChPT was performed in Ref. [40], and the mixing parameters were obtained from a fit to data from lattice QCD and input from the two-photon

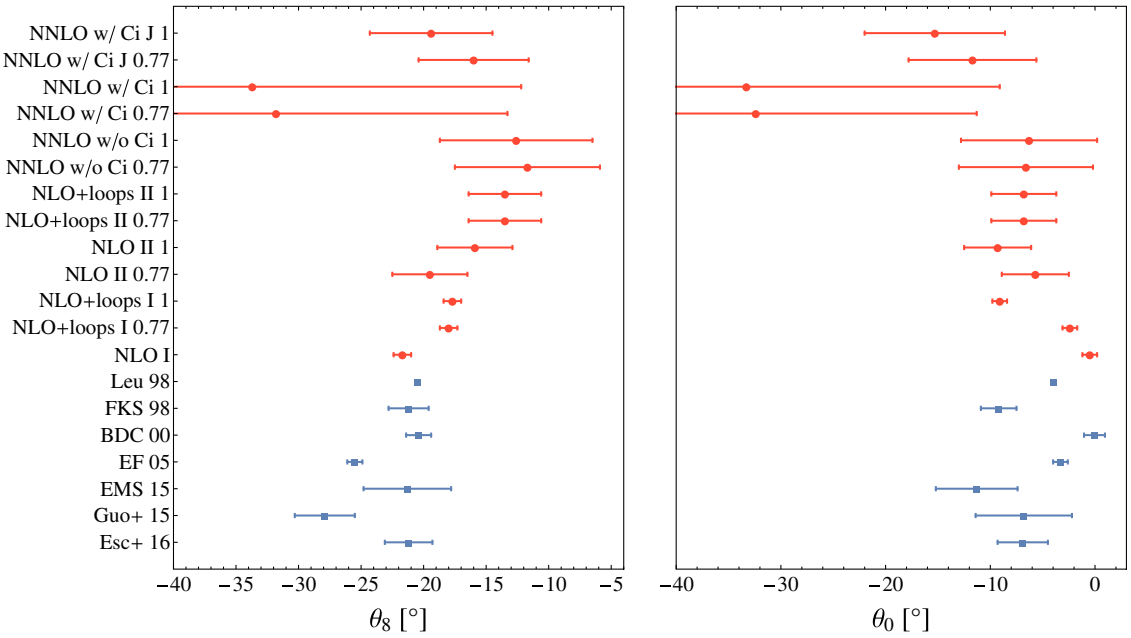

FIG. 7. Results for θ_8 and θ_0 obtained within the different scenarios in this work and compared to phenomenological determinations from Leutwyler (Leu 98) [36], Feldmann *et al.* (FKS 98) [45], Benayoun *et al.* (BDC 00) [47], Escribano and Frere (EF 05) [48], Escribano *et al.* (EMS 15) [51], Guo *et al.* (Guo + 15) [40], and Escribano *et al.* (Esc + 16) [52].

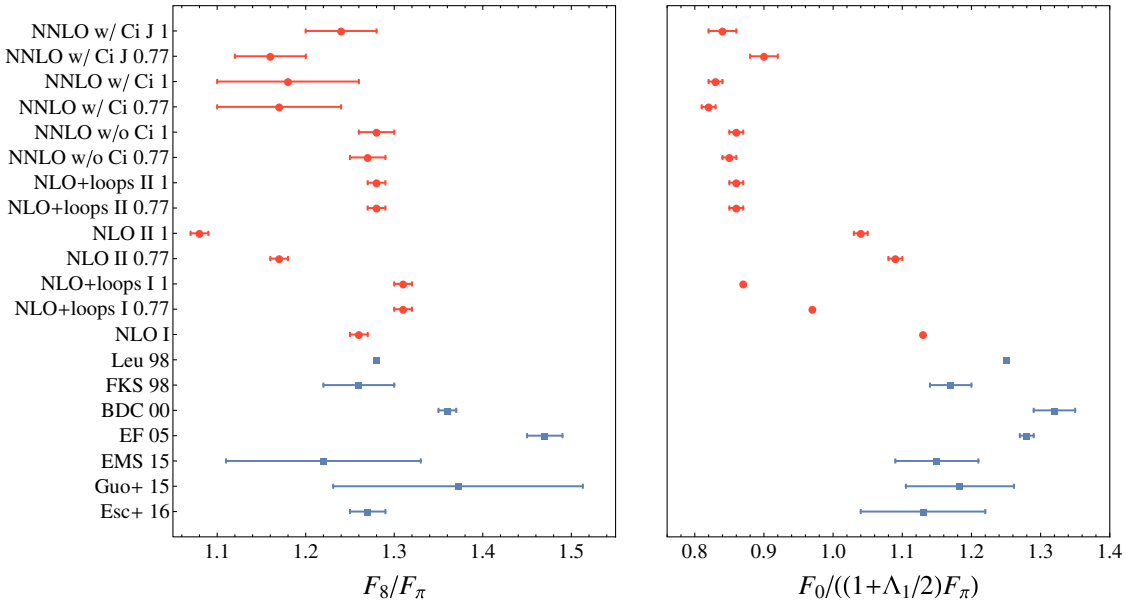

FIG. 8. Results for F_8 and $F_0/(1+\Lambda_1/2)$ obtained within the different scenarios in this work and compared to phenomenological determinations from (using the same abbreviations as defined in Fig. 7's caption) Leu 98 [36], FKS 98 [45], BDC 00 [47], EF 05 [48], EMS 15 [51], Guo + 15 [40], and Esc + 16 [52].

decays. However, the authors of Ref. [40] were also not able to determine all LECs at NNLO, and, therefore, they put some of the LECs to zero. For θ_0, in the cases without C_i, we find values between $-10°$ and $0°$, which agree approximately with the other calculations. For θ_8, the values in these cases range from $-22°$ to $-11°$, and their absolute values are slightly smaller than those obtained from phenomenology at NLO. Also, the NNLO w/ Ci J values for θ_8 and θ_0 tend to agree with the other scenarios and determinations. Again, the NNLO w/ Ci scenario is an exception, with values for θ_8 and θ_0 around $-33°$. These large negative values are related to the similar values for θ in this case and strongly depend on the C_i. Our values for F_8 agree with most of the other calculations. Note that F_8 depends only on LECs which appear in SU(3) ChPT as well and F_8 is not affected by neglecting unknown OZI rule-violating LECs. The errors of F_8 and $F_0/(1+\Lambda_1/2)$ due to the errors of the input parameters are very small, and the variation of our values in the different scenarios could serve as a better estimate of our systematic errors. For $F_0/(1+\Lambda_1/2)$, we find smaller values than the other works. The constant F_0 depends on the OZI rule-violating couplings Λ_1, L_{18}, and $L_{46}+L_{53}$. In our NNLO scenarios, however, all of them are set to zero, since they cannot be determined independently from the observables we study. Allowing values for Λ_1 and L_{18} which are different from zero, e.g., $\Lambda_1 \approx 0.3$ and $L_{18} \approx 0.3 \times 10^{-3}$, shifts F_0 to higher values in the range of the determinations of the other works. The values for F are mostly smaller than the physical value. This is consistent with the findings in Ref. [44].

The NLO I case is the most consistent scenario, since it is a full calculation up to NLO in LN_cChPT and does not rely on input from other theories with different degrees of freedom or a different power-counting scheme. However, our aim was a calculation of the mixing at the one-loop level up to NNLO in the δ counting. Among these scenarios, the most complete one is NNLO w/ Ci. Note that, even in this case, we could not fix all parameters and set five OZI rule-violating LECs equal to zero.

VI. SUMMARY AND OUTLOOK

We have derived an expression for the η-η' mixing in the framework of LN_cChPT up to NNLO, including higher-derivative, kinetic, and mass terms. Furthermore, we have calculated the axial-vector-current decay constants of the η-η' system at NNLO and determined the mixing parameters F_8, F_0, θ_8, and θ_0 of the two-angle scheme.

The numerical evaluation of the results has been performed successively at LO, NLO, and NNLO. At NLO, we have determined all LECs by fixing them to the physical values of the pseudoscalar masses M_π^2, M_K^2, M_η^2, and $M_{\eta'}^2$, the decay constants F_π and F_K, and the quark-mass ratio m_s/m. We have compared our results with the values for the LECs obtained in SU(3) ChPT [44]. Due to the large number of LECs at NNLO, we have not been able to determine all of them through our aforementioned input quantities. Therefore, we have made use of the values obtained in SU(3) ChPT and have applied the matching relations between SU(3) and U(3) ChPT. One OZI rule-violating parameter, L_{25}, has been fixed to the physical value of M_η^2. The impact of OZI rule-violating parameters on our observables is rather large, and they cannot be neglected. In addition to using input from SU(3) ChPT, we also

investigated the case where we employed LECs which were computed in a chiral quark model [69]. We have compared our results for the parameters of the two-angle scheme with other phenomenological determinations of those quantities.

The mixing angle θ and the angles θ_8 and θ_0 of the two-angle scheme depend strongly on the values of the NNLO corrections given by C_i terms. This leads to results which deviate very much from the determinations at LO, NLO, or NNLO without C_i terms. From this observation, we conclude that the mixing angles are particularly sensitive to the expansion scheme, and it remains unclear to which extent the convergence is under control.

At NNLO, it has not been possible to determine all LECs from the available experimental data. In the future, lattice QCD may provide further information on these LECs, since it will make it possible to study the quark-mass dependence of the pseudoscalar masses and decay constants.

Our NNLO expressions for the η-η' mixing can now be used to study anomalous decays, e.g. $\eta^{(\prime)} \to \gamma\gamma$ and $\eta^{(\prime)} \to \pi^+\pi^-\gamma$, consistently at the one-loop level. A further step would be the inclusion of vector mesons as explicit degrees of freedom and the investigation of $PV\gamma$ processes, where P refers to pseudoscalar mesons and V to vector mesons.

ACKNOWLEDGMENTS

Supported by the Deutsche Forschungsgemeinschaft through the Collaborative Research Center "The Low-Energy Frontier of the Standard Model" (SFB 1044). P. M. wants to thank G. Ecker and J. J. Sanz-Cillero for useful discussions.

APPENDIX A: BUILDING BLOCKS AND TRANSFORMATION BEHAVIOR

The effective dynamical degrees of freedom are contained in the U(3) matrix

$$U = \exp\left(i\sum_{a=0}^{8}\frac{\phi_a\lambda_a}{F}\right) = e^{\frac{i}{3}\psi}\hat{U},$$

where

$$\det(\hat{U}) = 1, \qquad \det(U) = e^{i\psi}, \qquad \psi = -i\ln(\det(U)).$$

The external fields s, p, l_μ, and r_μ are Hermitian, color-neutral 3×3 matrices coupling to the corresponding quark bilinears, and θ is a real field coupling to the winding-number density [27]. The traceless components of r_μ and l_μ are defined as

$$r_\mu = \hat{r}_\mu + \frac{1}{3}\langle r_\mu\rangle, \qquad \langle\hat{r}_\mu\rangle = 0,$$
$$l_\mu = \hat{l}_\mu + \frac{1}{3}\langle l_\mu\rangle, \qquad \langle\hat{l}_\mu\rangle = 0.$$

We parametrize the group elements $(V_L, V_R) \in \mathrm{U}(3)_L \times \mathrm{U}(3)_R$ in terms of

$$V_R = \exp\left(-i\sum_{a=0}^{8}\theta_{Ra}\frac{\lambda_a}{2}\right) = e^{-\frac{i}{3}\theta_R}\hat{V}_R,$$
$$\det(\hat{V}_R) = 1, \qquad \theta_R = i\ln(\det(V_R)),$$
$$V_L = \exp\left(-i\sum_{a=0}^{8}\theta_{La}\frac{\lambda_a}{2}\right) = e^{-\frac{i}{3}\theta_L}\hat{V}_L,$$
$$\det(\hat{V}_L) = 1, \qquad \theta_L = i\ln(\det(V_L)).$$

We define $v_\mu = \frac{1}{2}(r_\mu + l_\mu)$, $a_\mu = \frac{1}{2}(r_\mu - l_\mu)$, and $\chi = 2B(s+ip)$. Under the group $G = \mathrm{U}(3)_L \times \mathrm{U}(3)_R$, the transformation properties of the dynamical degrees of freedom and of the external fields read

$$\begin{aligned}
U &\mapsto V_R U V_L^\dagger,\\
\psi &\mapsto \psi - i\ln(\det(V_R)) + i\ln(\det(V_L))\\
&= \psi - (\theta_R - \theta_L),\\
r_\mu &\mapsto V_R r_\mu V_R^\dagger + iV_R\partial_\mu V_R^\dagger,\\
\hat{r}_\mu &\mapsto \hat{V}_R\hat{r}_\mu\hat{V}_R^\dagger + i\hat{V}_R\partial_\mu\hat{V}_R^\dagger,\\
\langle r_\mu\rangle &\mapsto \langle r_\mu\rangle - \partial_\mu\theta_R,\\
l_\mu &\mapsto V_L l_\mu V_L^\dagger + iV_L\partial_\mu V_L^\dagger,\\
\hat{l}_\mu &\mapsto \hat{V}_L\hat{l}_\mu\hat{V}_L^\dagger + i\hat{V}_L\partial_\mu\hat{V}_L^\dagger,\\
\langle l_\mu\rangle &\mapsto \langle l_\mu\rangle - \partial_\mu\theta_L,\\
\langle a_\mu\rangle &\mapsto \langle a_\mu\rangle - \frac{1}{2}(\partial_\mu\theta_R - \partial_\mu\theta_L),\\
\chi &\mapsto V_R\chi V_L^\dagger,\\
\theta &\mapsto \theta + (\theta_R - \theta_L).
\end{aligned} \tag{A1}$$

We define covariant derivatives according to the transformation behavior of the object to which they are applied:

$$\begin{aligned}
D_\mu U &= \partial_\mu U - ir_\mu U + iUl_\mu \mapsto V_R D_\mu U V_L^\dagger,\\
D_\mu U^\dagger &= \partial_\mu U^\dagger + iU^\dagger r_\mu - il_\mu U^\dagger \mapsto V_L D_\mu U^\dagger V_R^\dagger,\\
D_\mu\hat{U} &= \partial_\mu\hat{U} - i\hat{r}_\mu\hat{U} + i\hat{U}\hat{l}_\mu,\\
D_\mu\psi &= \partial_\mu\psi - 2\langle a_\mu\rangle \mapsto D_\mu\psi,\\
D_\mu U &= e^{\frac{i}{3}\psi}\left(D_\mu\hat{U} + \frac{i}{3}D_\mu\Psi\hat{U}\right),\\
D_\mu\theta &= \partial_\mu\theta + 2\langle a_\mu\rangle \mapsto D_\mu\theta.
\end{aligned} \tag{A2}$$

Finally, the parity transformation behavior reads

$$\begin{aligned}
U(t,\vec{x}) &\mapsto U^\dagger(t,-\vec{x}),\\
\psi(t,\vec{x}) &\mapsto -\psi(t,-\vec{x}),\\
\theta(t,\vec{x}) &\mapsto -\theta(t,-\vec{x}),\\
D_\mu U(t,\vec{x}) &\mapsto D^\mu U^\dagger(t,-\vec{x}).
\end{aligned}$$

APPENDIX B: MASSES AND DECAY CONSTANTS

The pion-decay constant F in the chiral limit is given by

$$F = F_\pi\left[1 - \frac{4M_\pi^2 L_5}{F_\pi^2} - \frac{1}{F_\pi^4}(4(2M_\pi^4(3(L_5)^2 - 8L_8L_5 + (C_{14}+C_{17})F_\pi^2) + F_\pi^2(2M_K^2 + M_\pi^2)L_4)) - \frac{A_0(M_K^2) + 2A_0(M_\pi^2)}{32\pi^2F_\pi^2}\right] \tag{B1}$$

in terms of the physical decay constant F_π and the physical pion and kaon masses, M_π and M_K, respectively. The expression for the LO pion mass $\overset{\circ}{M}{}_\pi^2$ reads

$$\begin{aligned}\overset{\circ}{M}{}_\pi^2 &= 2B\hat{m}\\ &= M_\pi^2\Bigg[1 + \frac{8M_\pi^2(L_5 - 2L_8)}{F_\pi^2} + \frac{1}{F_\pi^4}(8(2M_\pi^4(8(L_5-2L_8)^2 + (2C_{12}+C_{14}+C_{17}-3C_{19}-2C_{31})F_\pi^2)\\ &\quad + 2F_\pi^2M_K^2(L_4-2L_6) + F_\pi^2M_\pi^2(L_4-2L_6)))\\ &\quad + \frac{1}{192F_\pi^2}((2\sqrt{2}\sin(2\theta^{[0]}) + \cos(2\theta^{[0]}) - 3)A_0(M_\eta^2) - (2\sqrt{2}\sin(2\theta^{[0]}) + \cos(2\theta^{[0]}) + 3)A_0(M_{\eta'}^2) + 6A_0(M_\pi^2))\Bigg],\end{aligned} \tag{B2}$$

and the LO kaon mass $\overset{\circ}{M}{}_K^2$ is given by

$$\begin{aligned}\overset{\circ}{M}{}_K^2 &= B(\hat{m} + ms)\\ &= M_K^2\Bigg[1 + \frac{8M_K^2(L_5 - 2L_8)}{F_\pi^2} + \frac{1}{F_\pi^4}(8(4M_K^4(2(L_5-4L_8)(L_5-2L_8) + (C_{12}+C_{14}-3C_{19}-C_{31})F_\pi^2)\\ &\quad + 2M_K^2(F_\pi^2(L_4 - 2L_6 + 2(-C_{14}+C_{17}+3C_{19})M_\pi^2) + 4M_\pi^2L_5(L_5-2L_8))\\ &\quad - F_\pi^2M_\pi^2(2(L_6 + (-C_{14}+C_{17}+3C_{19})M_\pi^2) - L_4)))\\ &\quad + \frac{1}{192F_\pi^2M_K^2}(\sin^2(\theta^{[0]})((3M_{\eta'}^2 + M_\pi^2)A_0(M_{\eta'}^2) - 4M_K^2A_0(M_\eta^2))\\ &\quad + \sqrt{2}(2M_K^2 - M_\pi^2)\sin(2\theta^{[0]})(A_0(M_{\eta'}^2) - A_0(M_\eta^2)) + \cos^2(\theta^{[0]})((3M_\eta^2 + M_\pi^2)A_0(M_\eta^2) - 4M_K^2A_0(M_{\eta'}^2)))\Bigg].\end{aligned} \tag{B3}$$

In loop contributions, we always use the LO mixing angle

$$\theta^{[0]} = -\arctan\left(\frac{2\sqrt{2}(M_K^2 - M_\pi^2)}{3(\frac{1}{3}(M_\pi^2 - 4M_K^2) + M_{\eta'}^2)}\right), \tag{B4}$$

which yields $\theta^{[0]} = -19.6°$. The ratio of the physical kaon-decay and pion-decay constants is given by

$$\begin{aligned}F_K/F_\pi &= 1 + \frac{4(M_K^2 - M_\pi^2)L_5}{F_\pi^2} + \frac{1}{F_\pi^4}(8((3M_K^4 + 2M_\pi^2M_K^2 - 3M_\pi^4)(L_5)^2 + 8(M_\pi^4 - M_K^4)L_8L_5\\ &\quad + 2F_\pi^2(M_K^2 - M_\pi^2)(C_{14}M_K^2 + C_{17}M_\pi^2)))\\ &\quad + \frac{1}{128\pi^2F_\pi^2}(2A_0(M_K^2) + 3\cos^2(\theta^{[0]})A_0(M_\eta^2) + 3\sin^2(\theta^{[0]})A_0(M_{\eta'}^2) - 5A_0(M_\pi^2)).\end{aligned} \tag{B5}$$

The NNLO expressions for the decay constants of the η-η' system are given by

$$
\begin{aligned}
F_\eta^8 = {} & F_\pi \cos(\theta^{[2]}) + \frac{1}{3F_\pi}(8(M_K^2 - M_\pi^2)L_5(\sqrt{2}\sin(\theta^{[2]}) + 2\cos(\theta^{[2]}))) \\
& + \frac{\cos(\theta^{[2]})}{48\pi^2 F_\pi^3}[256\pi^2((4M_K^4 + 8M_\pi^2 M_K^2 - 9M_\pi^4)(L_5)^2 + 16(M_\pi^4 - M_K^4)L_8 L_5 + 4(C_{14} + C_{17})F_\pi^2 M_K^2(M_K^2 - M_\pi^2)) \\
& + 3F_\pi^2(A_0(M_K^2) - A_0(M_\pi^2))] \\
& + \frac{\sin(\theta^{[2]})}{3F_\pi^3}[2\sqrt{2}(M_K^2 - M_\pi^2)(F_\pi^2(-\Lambda_1 L_5 + 16(C_{14} + C_{17})M_K^2 + 6L_{18}) + 16L_5((M_K^2 + 3M_\pi^2)L_5 - 4(M_K^2 + M_\pi^2)L_8))] \\
& + \frac{C_{12}}{3F_\pi(4M_K^2 - 3M_{\eta'}^2 - M_\pi^2)}[16(M_K^2 - M_\pi^2)(-2(M_K^2 - M_\pi^2)M_{\eta'}^2(\sqrt{2}\sin(\theta^{[2]}) - 4\cos(\theta^{[2]})) \\
& + 3\sqrt{2}M_\pi^2(M_\pi^2 - 2M_K^2)\sin(\theta^{[2]}) + 3\sqrt{2}M_{\eta'}^4\sin(\theta^{[2]}))],
\end{aligned}
\tag{B6}
$$

$$
\begin{aligned}
F_{\eta'}^8 = {} & F_\pi \sin(\theta^{[2]}) - \frac{1}{3F_\pi}(8(M_K^2 - M_\pi^2)L_5(\sqrt{2}\cos(\theta^{[2]}) - 2\sin(\theta^{[2]}))) \\
& - \frac{\cos(\theta^{[2]})}{3F_\pi^3}[2\sqrt{2}(M_K^2 - M_\pi^2)(F_\pi^2(-\Lambda_1 L_5 + 16(C_{14} + C_{17})M_K^2 + 6L_{18}) + 16L_5((M_K^2 + 3M_\pi^2)L_5 - 4(M_K^2 + M_\pi^2)L_8))] \\
& + \frac{\sin(\theta^{[2]})}{48\pi^2 F_\pi^3}[256\pi^2((4M_K^4 + 8M_\pi^2 M_K^2 - 9M_\pi^4)(L_5)^2 + 16(M_\pi^4 - M_K^4)L_8 L_5 \\
& + 4(C_{14} + C_{17})F_\pi^2 M_K^2(M_K^2 - M_\pi^2)) + 3F_\pi^2(A_0(M_K^2) - A_0(M_\pi^2))] \\
& + \frac{C_{12}}{3F_\pi}\left[16\left(\frac{1}{4M_K^2 - 3M_{\eta'}^2 - M_\pi^2}[\sqrt{2}(M_K^2 - M_\pi^2)\cos(\theta^{[2]})(-2M_K^2(7M_{\eta'}^2 + 5M_\pi^2) + 16M_K^4 + 3M_{\eta'}^4 + 2M_\pi^2 M_{\eta'}^2 + 3M_\pi^4\right)\right] \\
& - \sin(\theta^{[2]})(-4M_K^2(M_{\eta'}^2 + 2M_\pi^2) + 8M_K^4 + M_\pi^2(M_{\eta'}^2 + 3M_\pi^2)))],
\end{aligned}
\tag{B7}
$$

$$
\begin{aligned}
F_\eta^0 = {} & -\frac{1}{6F_\pi}[16(M_K^2 - M_\pi^2)L_5(\sin(\theta^{[2]}) + \sqrt{2}\cos(\theta^{[2]})) + 3F_\pi^2(\Lambda_1 + 2)\sin(\theta^{[2]})] \\
& - \frac{\cos(\theta^{[2]})}{3F_\pi^3}[2\sqrt{2}(M_K^2 - M_\pi^2)(F_\pi^2(-\Lambda_1 L_5 + 16(C_{14} + C_{17})M_K^2 \\
& + 6(L_{18} + 2L_{46} + 2L_{53})) + 16L_5((M_K^2 + 3M_\pi^2)L_5 - 4(M_K^2 + M_\pi^2)L_8))] \\
& + \frac{\sin(\theta^{[2]})}{96\pi^2 F_\pi^3}[2(2\pi^2(32(4L_5(8(M_K^4 - M_\pi^4)L_8 + (-2M_K^4 - 4M_\pi^2 M_K^2 + 3M_\pi^4)L_5) \\
& + F_\pi^2(M_\pi^2(8(C_{14} + C_{17})M_K^2 - 3(L_{18} + L_{46} + L_{53})) - 8(C_{14} + C_{17})M_K^4 \\
& - 6(L_{18} + L_{46} + L_{53})M_K^2)) + 32F_\pi^2\Lambda_1(M_K^2 + 2M_\pi^2)L_5 + 3F_\pi^4\Lambda_1^2) + 3F_\pi^2 A_0(M_\pi^2)) + 3F_\pi^2 A_0(M_K^2)] \\
& + \frac{C_{12}}{3F_\pi(4M_K^2 - 3M_{\eta'}^2 - M_\pi^2)}[16(\sin(\theta^{[2]})(4M_K^2 - 3M_{\eta'}^2 - M_\pi^2) \\
& \times (2M_K^2(M_{\eta'}^2 - 3M_\pi^2) + M_\pi^2(M_{\eta'}^2 + 3M_\pi^2)) + \sqrt{2}(M_K^2 - M_\pi^2)\cos(\theta^{[2]}) \\
& \times (2M_K^2(M_{\eta'}^2 + 3M_\pi^2) - 2M_\pi^2 M_{\eta'}^2 - 3M_{\eta'}^4 - 3M_\pi^4))],
\end{aligned}
\tag{B8}
$$

$$F^0_{\eta'} = \frac{1}{6F_\pi}[16(M_K^2 - M_\pi^2)L_5(\cos(\theta^{[2]}) - \sqrt{2}\sin(\theta^{[2]})) + 3F_\pi^2(\Lambda_1 + 2)\cos(\theta^{[2]})]$$
$$\times \frac{\cos(\theta^{[2]})}{96\pi^2 F_\pi^3}[2(2\pi^2(32(4L_5((2M_K^4 + 4M_\pi^2 M_K^2 - 3M_\pi^4)L_5 + 8(M_\pi^4 - M_K^4)L_8)$$
$$+ F_\pi^2(M_\pi^2(3(L_{18} + L_{46} + L_{53}) - 8(C_{14} + C_{17})M_K^2) + 8(C_{14} + C_{17})M_K^4 + 6(L_{18} + L_{46} + L_{53})M_K^2))$$
$$- 32F_\pi^2\Lambda_1(M_K^2 + 2M_\pi^2)L_5 - 3F_\pi^4\Lambda_1^2) - 3F_\pi^2 A_0(M_\pi^2)) - 3F_\pi^2 A_0(M_K^2)]$$
$$- \frac{\sin(\theta^{[2]})}{3F_\pi^3}[2\sqrt{2}(M_K^2 - M_\pi^2)(F_\pi^2(-\Lambda_1 L_5 + 16(C_{14} + C_{17})M_K^2 + 6(L_{18} + 2L_{46} + 2L_{53})) + 16L_5((M_K^2 + 3M_\pi^2)L_5$$
$$- 4(M_K^2 + M_\pi^2)L_8))] + \frac{C_{12}}{3F_\pi(4M_K^2 - 3M_{\eta'}^2 - M_\pi^2)}[16(M_K^2 - M_\pi^2)(\sqrt{2}\sin(\theta^{[2]})$$
$$\times(-2M_K^2(7M_{\eta'}^2 + 5M_\pi^2) + 16M_K^4 + 3M_{\eta'}^4 + 2M_\pi^2 M_{\eta'}^2 + 3M_\pi^4) - 8(M_K^2 - M_\pi^2)\cos(\theta^{[2]})(2M_K^2 - M_{\eta'}^2))], \tag{B9}$$

in terms of the physical masses M_π^2, M_K^2, and $M_{\eta'}^2$ and the physical pion-decay constant F_π. The mixing angle $\theta^{[2]}$ is the NNLO mixing angle given in Eq. (49) in Sec. III. In the case where the loop contributions are added to the NLO results, the parameters of the two-angle scheme can be simplified to read

$$F_8 = F_\pi + \frac{1}{48\pi^2 F_\pi}[256\pi^2(M_K^2 - M_\pi^2)L_5 + 3A_0(M_K^2) - 3A_0(M_\pi^2)], \tag{B10}$$

$$F_0 = F_\pi + \frac{1}{96\pi^2 F_\pi}[16\pi^2(16M_K^2(L_5 + 3L_{18}) + 8M_\pi^2(3L_{18} - 2L_5) + 3F_\pi^2\Lambda_1) - 3A_0(M_K^2) - 6A_0(M_\pi^2)], \tag{B11}$$

$$\theta_8 = \theta^{[2]} + \arctan\left(-\frac{4\sqrt{2}(M_K^2 - M_\pi^2)(2L_5 + 3L_{18})}{3F_\pi^2}\right), \tag{B12}$$

$$\theta_0 = \theta^{[2]} - \arctan\left(-\frac{4\sqrt{2}(M_K^2 - M_\pi^2)(2L_5 + 3L_{18})}{3F_\pi^2}\right). \tag{B13}$$

APPENDIX C: KINETIC MATRIX AND MASS MATRIX AT NNLO

In the following, the NNLO expressions for the matrix $\mathcal{C}_A$ defined in Eq. (18) in Sec. III, the kinetic matrix $\mathcal{K}_B$, and the mass matrix $\mathcal{M}_B$ defined in Eq. (27) are provided. The components of $\mathcal{C}_A$ are given by

$$c_8 = \frac{32C_{12}(4M_K^2 - M_\pi^2)}{3F_\pi^2}, \tag{C1}$$

$$c_1 = \frac{32C_{12}(2M_K^2 + M_\pi^2)}{3F_\pi^2}, \tag{C2}$$

$$c_{81} = \frac{64\sqrt{2}C_{12}(M_\pi^2 - M_K^2)}{3F_\pi^2}. \tag{C3}$$

At NNLO, both tree and loop corrections occur. The second-order tree contributions to the kinetic matrix read

$$\delta_8^{(2,\mathrm{tr})} = \frac{1}{3F_\pi^4}[8(2(8(2M_K^4 + 2M_\pi^2 M_K^2 - M_\pi^4)(L_5)^2 + 8(M_\pi^4 - 4M_K^4)L_8 L_5 + (C_{14} + C_{17})F_\pi^2(8M_K^4 - 8M_\pi^2 M_K^2 + 3M_\pi^4))$$
$$+ 3F_\pi^2(2M_K^2 + M_\pi^2)L_4) + 32C_{12}F_\pi^2(8M_K^4 - 8M_\pi^2 M_K^2 + 3M_\pi^4)], \tag{C4}$$

$$\delta_1^{(2,\mathrm{tr})} = \frac{1}{3F_\pi^4}[8(3F_\pi^2(2M_K^2 + M_\pi^2)L_4 + 16(M_K^4 + M_\pi^2 M_K^2 + M_\pi^4)(L_5)^2 - 16(2M_K^4 + M_\pi^4)L_8 L_5$$
$$+ 2(C_{14} + C_{17})(4M_K^4 - 4M_\pi^2 M_K^2 + 3M_\pi^4) + 3L_{18}(2M_K^2 + M_\pi^2)))$$
$$+ 32C_{12}F_\pi^2(4M_K^4 - 4M_\pi^2 M_K^2 + M_0^2(2M_K^2 + M_\pi^2) + 3M_\pi^4)], \tag{C5}$$

$$\delta_{81}^{(2,\mathrm{tr})} = -\frac{1}{3F_\pi^4}[8\sqrt{2}(M_K^2 - M_\pi^2)(16L_5((M_K^2 + 2M_\pi^2)L_5 - 2(M_K^2 + M_\pi^2)L_8) + F_\pi^2(8(C_{14} + C_{17})M_K^2 + 3L_{18}))$$
$$+ 32\sqrt{2}C_{12}F_\pi^2(4M_K^2 + M_0^2)(M_K^2 - M_\pi^2)], \tag{C6}$$

and the loop contributions read

$$\delta_8^{(2,\mathrm{lo})} = \frac{A_0(M_K^2)}{16\pi^2 F_\pi^2}, \qquad \delta_1^{(2,\mathrm{lo})} = 0, \qquad \delta_{81}^{(2,\mathrm{lo})} = 0. \tag{C7}$$

The second-order tree contributions to the mass matrix are

$$\begin{aligned}\Delta M_8^{2\,(2,\mathrm{tr})} = \frac{1}{3F_\pi^4}[&16(16M_K^6(8(L_5-2L_8)L_8+(3C_{19}+2C_{31})F_\pi^2)+8M_\pi^2M_K^4(16(L_8)^2-3(3C_{19}+2C_{31})F_\pi^2)\\&+4M_\pi^4M_K^2(32L_8(L_8-L_5)+3(3C_{19}+2C_{31})F_\pi^2)+M_\pi^6(24(3L_5-4L_8)L_8-(3C_{19}+2C_{31})F_\pi^2)\\&+8F_\pi^2(M_K^2-M_\pi^2)^2L_7+F_\pi^2(8M_K^4+2M_\pi^2M_K^2-M_\pi^4)L_6)],\end{aligned} \tag{C8}$$

$$\begin{aligned}\Delta M_1^{2\,(2,\mathrm{tr})} = \frac{1}{3F_\pi^4}[&16(F_\pi^2\Lambda_2(2M_K^4+M_\pi^4)(L_5-2L_8)+F_\pi^2(2M_K^2+M_\pi^2)^2L_6+F_\pi^2(2M_K^2+M_\pi^2)^2L_7-128M_K^6(L_8)^2\\&+64M_K^6L_5L_8+64M_\pi^2M_K^4(L_8)^2+64M_\pi^4M_K^2(L_8)^2-64M_\pi^4M_K^2L_5L_8-96M_\pi^6(L_8)^2+72M_\pi^6L_5L_8\\&+24C_{19}F_\pi^2M_K^6+16C_{31}F_\pi^2M_K^6-36C_{19}F_\pi^2M_\pi^2M_K^4-24C_{31}F_\pi^2M_\pi^2M_K^4+18C_{19}F_\pi^2M_\pi^4M_K^2+12C_{31}F_\pi^2M_\pi^4M_K^2\\&+3C_{19}F_\pi^2M_\pi^6+2C_{31}F_\pi^2M_\pi^6-12F_\pi^2L_{25}M_K^4+12F_\pi^2L_{25}M_\pi^2M_K^2-9F_\pi^2L_{25}M_\pi^4)]+6(2M_K^2+M_\pi^2)v_2^{(2)},\end{aligned} \tag{C9}$$

$$\begin{aligned}\Delta M_{81}^{2\,(2,\mathrm{tr})} = -\frac{1}{3F_\pi^4}[&16\sqrt{2}(M_K^2-M_\pi^2)(2(4M_K^4(8(L_5-2L_8)L_8+(3C_{19}+2C_{31})F_\pi^2)\\&+M_\pi^2(F_\pi^2(L_6+L_7-2(3C_{19}+2C_{31})M_K^2)+32M_K^2(L_5-L_8)L_8)\\&+F_\pi^2M_K^2(2(L_6+L_7)-3L_{25})+(3C_{19}+2C_{31})F_\pi^2M_\pi^4)+F_\pi^2\Lambda_2(M_K^2+M_\pi^2)(L_5-2L_8))],\end{aligned} \tag{C10}$$

and the loop corrections are given by

$$\begin{aligned}\Delta M_8^{2\,(2,\mathrm{lo})} = \frac{1}{576F_\pi^2}(&2\sqrt{2}(8M_K^2-5M_\pi^2)\sin(2\theta^{[0]})(A_0(M_\eta^2)-A_0(M_{\eta'}^2))+(8M_K^2-5M_\pi^2)\cos(2\theta^{[0]})(A_0(M_\eta^2)-A_0(M_{\eta'}^2))\\&+3(8M_K^2-3M_\pi^2)(A_0(M_\eta^2)+A_0(M_{\eta'}^2))+6M_\pi^2(3A_0(M_\pi^2)-2A_0(M_K^2))),\end{aligned} \tag{C11}$$

$$\begin{aligned}\Delta M_1^{2\,(2,\mathrm{lo})} = \frac{1}{144F_\pi^2}(&2\sqrt{2}(M_K^2-M_\pi^2)\sin(2\theta^{[0]})(A_0(M_\eta^2)-A_0(M_{\eta'}^2))+(M_K^2-M_\pi^2)\cos(2\theta^{[0]})(A_0(M_\eta^2)-A_0(M_{\eta'}^2))\\&+3M_K^2(4A_0(M_K^2)+A_0(M_\eta^2)+A_0(M_{\eta'}^2))+9M_\pi^2A_0(M_\pi^2)),\end{aligned} \tag{C12}$$

$$\begin{aligned}\Delta M_{81}^{2\,(2,\mathrm{lo})} = \frac{1}{576F_\pi^2}(&4(4M_K^2-M_\pi^2)\sin(2\theta^{[0]})(A_0(M_{\eta'}^2)-A_0(M_\eta^2))+\sqrt{2}(4M_K^2-M_\pi^2)\cos(2\theta^{[0]})(A_0(M_{\eta'}^2)-A_0(M_\eta^2))\\&-3\sqrt{2}((4M_K^2-3M_\pi^2)(A_0(M_\eta^2)+A_0(M_{\eta'}^2))+(8M_K^2-4M_\pi^2)A_0(M_K^2)-6M_\pi^2A_0(M_\pi^2))).\end{aligned} \tag{C13}$$

APPENDIX D: INPUT PARAMETERS

TABLE XIV. Summary of the results for the LECs determined in the numerical analysis of the η-η' mixing in Sec. V.

	μ (GeV)	L_5 $[10^{-3}]$	L_8 $[10^{-3}]$	$\tilde{\Lambda}$	L_{25} $[10^{-3}]$
NLO I	⋯	1.86 ± 0.06	0.78 ± 0.05	-0.34 ± 0.05	0 ± 0
NLO + loops I	0.77	1.37 ± 0.06	0.85 ± 0.05	0.52 ± 0.05	0 ± 0
NLO + loops I	1	0.75 ± 0.06	0.55 ± 0.05	1.09 ± 0.04	0 ± 0
NLO II	0.77	1.20 ± 0.10	0.55 ± 0.20	0.02 ± 0.13	0 ± 0
NLO II	1	0.58 ± 0.10	0.24 ± 0.20	0.41 ± 0.13	0 ± 0
NLO + loops II	0.77	1.20 ± 0.10	0.55 ± 0.20	1.34 ± 0.13	0 ± 0
NLO + loops II	1	0.58 ± 0.10	0.24 ± 0.20	1.34 ± 0.13	0 ± 0
NNLO w/o Ci	0.77	1.20 ± 0.10	0.55 ± 0.20	0 ± 0	0.55 ± 0.08
NNLO w/o Ci	1	0.58 ± 0.10	0.24 ± 0.20	0 ± 0	0.50 ± 0.08
NNLO w/ Ci	0.77	1.01 ± 0.06	0.52 ± 0.10	0 ± 0	0.67 ± 0.13
NNLO w/ Ci	1	0.39 ± 0.06	0.21 ± 0.10	0 ± 0	0.63 ± 0.13
NNLO w/ Ci J	0.77	1.26 ± 0.06	0.84 ± 0.05	0 ± 0	0.70 ± 0.07
NNLO w/ Ci J	1	1.26 ± 0.06	0.84 ± 0.05	0 ± 0	0.77 ± 0.07

TABLE XV. Input LECs used in Sec. V.

	μ (GeV)	L_4 $[10^{-3}]$	L_6 $[10^{-3}]$	L_7 $[10^{-3}]$	L_{18} $[10^{-3}]$
NLO I	⋯	0 ± 0	0 ± 0	0 ± 0	0 ± 0
NLO + loops I	0.77	0 ± 0	0 ± 0	0 ± 0	0 ± 0
NLO + loops I	1	0 ± 0	0 ± 0	0 ± 0	0 ± 0
NLO II	0.77	0 ± 0	0 ± 0	0 ± 0	0 ± 0
NLO II	1	0 ± 0	0 ± 0	0 ± 0	0 ± 0
NLO + loops II	0.77	0.21 ± 0	0.10 ± 0	0 ± 0	-0.41 ± 0
NLO + loops II	1	0 ± 0	0 ± 0	0 ± 0	0 ± 0
NNLO w/o Ci	0.77	0 ± 0.30	0.04 ± 0.40	0 ± 0.20	-0.41 ± 0
NNLO w/o Ci	1	-0.21 ± 0.30	-0.07 ± 0.40	0 ± 0.20	0 ± 0
NNLO w/ Ci	0.77	0.30 ± 0	0.18 ± 0.05	0 ± 0.09	-0.41 ± 0
NNLO w/ Ci	1	0.09 ± 0	0.07 ± 0.05	0 ± 0.09	0 ± 0
NNLO w/ Ci J	0.77	0 ± 0	0 ± 0	0 ± 0.05	0 ± 0
NNLO w/ Ci J	1	0 ± 0	0 ± 0	0 ± 0.05	0 ± 0

TABLE XVI. Input LECs used in Sec. V in GeV^{-2}.

	μ (GeV)	C_{12} $[10^{-3}]$	C_{14} $[10^{-3}]$	C_{17} $[10^{-3}]$	C_{19} $[10^{-3}]$	C_{31} $[10^{-3}]$
NLO I	⋯	0 ± 0	0 ± 0	0 ± 0	0 ± 0	0 ± 0
NLO + loops I	0.77	0 ± 0	0 ± 0	0 ± 0	0 ± 0	0 ± 0
NLO + loops I	1	0 ± 0	0 ± 0	0 ± 0	0 ± 0	0 ± 0
NLO II	0.77	0 ± 0	0 ± 0	0 ± 0	0 ± 0	0 ± 0
NLO II	1	0 ± 0	0 ± 0	0 ± 0	0 ± 0	0 ± 0
NLO + loops II	0.77	0 ± 0	0 ± 0	0 ± 0	0 ± 0	0 ± 0
NLO + loops II	1	0 ± 0	0 ± 0	0 ± 0	0 ± 0	0 ± 0
NNLO w/o Ci	0.77	0 ± 0	0 ± 0	0 ± 0	0 ± 0	0 ± 0
NNLO w/o Ci	1	0 ± 0	0 ± 0	0 ± 0	0 ± 0	0 ± 0
NNLO w/ Ci	0.77	-0.33 ± 0.16	-0.12 ± 0.06	-0.12 ± 0.06	-0.34 ± 0.24	0.63 ± 0.12
NNLO w/ Ci	1	-0.33 ± 0.16	-0.12 ± 0.06	-0.12 ± 0.06	-0.34 ± 0.24	0.63 ± 0.12
NNLO w/ Ci J	0.77	-0.34 ± 0.01	-0.87 ± 0.21	0.17 ± 0.04	-0.14 ± 0.13	-0.07 ± 0.13
NNLO w/ Ci J	1	-0.34 ± 0.01	-0.87 ± 0.21	0.17 ± 0.04	-0.14 ± 0.13	-0.07 ± 0.13

[1] K. A. Olive *et al.* (Particle Data Group Collaboration), Chin. Phys. C **38**, 090001 (2014).
[2] P. Adlarson *et al.*, arXiv:1204.5509.
[3] K. Kampf *et al.*, arXiv:1308.2575.
[4] P. Adlarson *et al.*, arXiv:1412.5451.
[5] S. L. Adler, Phys. Rev. **177**, 2426 (1969).
[6] J. S. Bell and R. Jackiw, Nuovo Cimento A **60**, 47 (1969).
[7] S. L. Adler and W. A. Bardeen, Phys. Rev. **182**, 1517 (1969).
[8] S. Scherer and M. R. Schindler, Lect. Notes Phys. **830**, 1 (2012).
[9] J. Goldstone, A. Salam, and S. Weinberg, Phys. Rev. **127**, 965 (1962).
[10] G. 't Hooft, Phys. Rev. Lett. **37**, 8 (1976).
[11] E. Witten, Nucl. Phys. **B156**, 269 (1979).
[12] G. Veneziano, Nucl. Phys. **B159**, 213 (1979).
[13] G. 't Hooft, Nucl. Phys. **B75**, 461 (1974).
[14] E. Witten, Nucl. Phys. **B160**, 57 (1979).
[15] R. K. Bhaduri, *Models of the Nucleon: From Quarks to Soliton* (Addison-Wesley, Redwood City, CA, 1988), Sec. 5.6.
[16] A. V. Manohar, in *Probing the Standard Model of Particle Interactions.* Proceedings of the Les Houches Summer School, Session 68, edited by R. Gupta, A. Morel, E. de Rafael, and F. David (Elsevier, Amsterdam, 1999), Pt. 1 and 2.
[17] S. R. Coleman and E. Witten, Phys. Rev. Lett. **45**, 100 (1980).
[18] C. Rosenzweig, J. Schechter, and C. G. Trahern, Phys. Rev. D **21**, 3388 (1980).
[19] E. Witten, Ann. Phys. (N.Y.) **128**, 363 (1980).
[20] P. Di Vecchia and G. Veneziano, Nucl. Phys. **B171**, 253 (1980).
[21] K. Kawarabayashi and N. Ohta, Nucl. Phys. **B175**, 477 (1980).
[22] P. Di Vecchia, F. Nicodemi, R. Pettorino, and G. Veneziano, Nucl. Phys. **B181**, 318 (1981).
[23] H. Leutwyler, Mod. Phys. Lett. A **28**, 1360014 (2013).
[24] C. Amsler, T. DeGrand, and B. Krusche, Quark Model, in Ref. [1], pp. 259–269.
[25] N. Isgur, Phys. Rev. D **13**, 122 (1976).
[26] H. Fritzsch and J. D. Jackson, Phys. Lett. **66B**, 365 (1977).
[27] J. Gasser and H. Leutwyler, Nucl. Phys. **B250**, 465 (1985).
[28] J. F. Donoghue, B. R. Holstein, and Y. C. R. Lin, Phys. Rev. Lett. **55**, 2766 (1985); **61**, 1527 (1988).
[29] F. J. Gilman and R. Kauffman, Phys. Rev. D **36**, 2761 (1987); **37**, 3348 (1988).
[30] J. Schechter, A. Subbaraman, and H. Weigel, Phys. Rev. D **48**, 339 (1993).
[31] A. Bramon, R. Escribano, and M. D. Scadron, Eur. Phys. J. C **7**, 271 (1999).
[32] B. Moussallam, Phys. Rev. D **51**, 4939 (1995).
[33] H. Leutwyler, Phys. Lett. B **374**, 163 (1996).
[34] P. Herrera-Siklody, J. I. Latorre, P. Pascual, and J. Taron, Nucl. Phys. **B497**, 345 (1997).
[35] R. Kaiser and H. Leutwyler, Eur. Phys. J. C **17**, 623 (2000).
[36] H. Leutwyler, Nucl. Phys. B, Proc. Suppl. **64**, 223 (1998).
[37] R. Kaiser and H. Leutwyler, in *Nonperturbative Methods in Quantum Field Theory* (World Scientific, Singapore, 1998).
[38] P. Herrera-Siklody, Phys. Lett. B **442**, 359 (1998).
[39] B. Borasoy, Eur. Phys. J. C **34**, 317 (2004).
[40] X. K. Guo, Z. H. Guo, J. A. Oller, and J. J. Sanz-Cillero, J. High Energy Phys. 06 (2015) 175.
[41] S. Peris and E. de Rafael, Phys. Lett. B **348**, 539 (1995).
[42] H. Georgi, Phys. Rev. D **49**, 1666 (1994).
[43] S. Peris, Phys. Lett. B **324**, 442 (1994).
[44] J. Bijnens and G. Ecker, Annu. Rev. Nucl. Part. Sci. **64**, 149 (2014).
[45] T. Feldmann, P. Kroll, and B. Stech, Phys. Rev. D **58**, 114006 (1998).
[46] T. Feldmann, P. Kroll, and B. Stech, Phys. Lett. B **449**, 339 (1999).
[47] M. Benayoun, L. DelBuono, and H. B. O'Connell, Eur. Phys. J. C **17**, 593 (2000).
[48] R. Escribano and J. M. Frere, J. High Energy Phys. 06 (2005) 029.
[49] R. Escribano, P. Masjuan, and J. J. Sanz-Cillero, J. High Energy Phys. 05 (2011) 094.
[50] R. Escribano, P. Masjuan, and P. Sanchez-Puertas, Phys. Rev. D **89**, 034014 (2014).
[51] R. Escribano, P. Masjuan, and P. Sanchez-Puertas, Eur. Phys. J. C **75**, 414 (2015).
[52] R. Escribano, S. Gonzàlez-Solis, P. Masjuan, and P. Sanchez-Puertas, Phys. Rev. D **94**, 054033 (2016).
[53] P. Ball, J. M. Frere, and M. Tytgat, Phys. Lett. B **365**, 367 (1996).
[54] C. E. Thomas, J. High Energy Phys. 10 (2007) 026.
[55] R. Escribano and J. Nadal, J. High Energy Phys. 05 (2007) 006.
[56] R. J. Crewther, P. Di Vecchia, G. Veneziano, and E. Witten, Phys. Lett. **88B**, 123 (1979); **91B**, 487(E) (1980).
[57] K. Ottnad, B. Kubis, U.-G. Meißner, and F.-K. Guo, Phys. Lett. B **687**, 42 (2010).
[58] H. W. Fearing and S. Scherer, Phys. Rev. D **53**, 315 (1996).
[59] J. H. Koch, V. Pascalutsa, and S. Scherer, Phys. Rev. C **65**, 045202 (2002).
[60] S. Scherer, Adv. Nucl. Phys. **27**, 277 (2003).
[61] J. Bijnens, G. Colangelo, and G. Ecker, J. High Energy Phys. 02 (1999) 020.
[62] T. Ebertshäuser, H. W. Fearing, and S. Scherer, Phys. Rev. D **65**, 054033 (2002).
[63] J. Bijnens, L. Girlanda, and P. Talavera, Eur. Phys. J. C **23**, 539 (2002).
[64] S. Z. Jiang, F. J. Ge, and Q. Wang, Phys. Rev. D **89**, 074048 (2014).
[65] S. Scherer and H. W. Fearing, Phys. Rev. D **52**, 6445 (1995).
[66] H. W. Fearing and S. Scherer, Phys. Rev. C **62**, 034003 (2000).
[67] S. Aoki *et al.*, Eur. Phys. J. C **74**, 2890 (2014).
[68] R. Kaiser, Nucl. Phys. B, Proc. Suppl. **174**, 97 (2007).
[69] S. Z. Jiang, Z. L. Wei, Q. S. Chen, and Q. Wang, Phys. Rev. D **92**, 025014 (2015).